

# Biochemistry

© Copyright 1990 by the American Chemical Society

*Volume 29, Number 37*

*September 18, 1990*

*Perspectives in Biochemistry*

## Additivity of Mutational Effects in Proteins

James A. Wells

*Protein Engineering Department, Genentech, Inc., 460 Point San Bruno Boulevard, South San Francisco, California 94080*

*Received April 19, 1990; Revised Manuscript Received May 29, 1990*

The energetics of virtually all binding functions in proteins is the culmination of a set of molecular interactions. For example, removal of a single molecular contact by a point mutation causes relatively small reductions (typically 0.5–5 kcal/mol) in the free energy of transition-state stabilization [for reviews see Fersht (1987) and Wells and Estell (1988)], protein–protein interactions [Laskowski et al., 1983; Ackers & Smith, 1985], or protein stability [for review see Matthews (1987)] compared to the overall free energy associated with these functional properties (usually 5–20 kcal/mol). Thus, it is possible to modulate protein function by mutation at many contact sites. In fact, to design large changes in function will often require mutation of more than one functional residue.

There is now a large data base for free energy changes that result when single mutants are combined. A review of these data shows that, in the majority of cases, the sum of the free energy changes derived from the single mutations is nearly equal to the free energy change measured in the multiple mutant. However, there are two major exceptions where such simple additivity breaks down. The first is where the mutated residues interact with each other, by direct contact or indirectly through electrostatic interactions or structural perturbations, so that they no longer behave independently. The second is where the mutation causes a change in mechanism or rate-limiting step of the reaction. It is important to note that the additive effects discussed here do not change the molecularity of their respective reactions. When the molecularity of the reaction changes [as in comparing the free energy of binding of one linked substrate (A-B) versus the sum of two fragments (A + plus B)], large deviations from simple additivity can result from entropic effects (Jencks, 1981). Although the focus here is on enzyme activity, similar conclusions may be drawn from mutations affecting protein-protein interactions, protein-DNA recognition, or protein stability. Some practical examples and applications are discussed.

## ADDITIVITY RELATIONSHIPS

The change in free energy of a functional property caused by a mutation at site X is typically expressed relative to that

of the wild-type protein as  $\Delta\Delta G_{00}$ . Such free energy changes for two single mutants (X and Y) can be related to those of a double mutant (designated X,Y) by eq 1 (Carter et al., 1984; Ackers & Smith, 1985). The  $\Delta G_1$  term (also called the

$$\Delta G_{\infty, \eta} = \Delta \Delta G_{\infty} + \Delta \Delta G_{\eta} + \Delta G_i \quad (1)$$

coupling energy; Carter et al., 1984) should reflect the extent to which the change in energy of interaction between sites X and Y affects the functional property measured. It is possible for  $\Delta G_1$  to be either positive or negative depending upon whether the interactions between the mutant side chains reduce or enhance the functional property measured. Furthermore, the  $\Delta G_1$  term should not exceed the free energy of interaction between side chains at sites X and Y except in cases where these mutations cause large structural perturbations. This was first applied to evaluating the functional independence of residues mutated in tyrosyl-tRNA synthetase (Carter et al., 1984). In one case the sum of the double  $\Delta G$  values for single mutants was equal to that of the double mutant, indicating the sites functioned independently; in another example there was a large discrepancy, suggesting the sites were interacting.

## SIMPLE ADDITIVITY IN TRANSITION-STATE BINDING INTERACTIONS

The strengths of noncovalent interactions are strongly dependent upon the nature of the two groups and the distance ( $r$ ) between them. For example, the free energy of charge-charge, random charge-dipole, random dipole-dipole, van der Waals attraction, and repulsion decay as  $1/r$ ,  $1/r^2$ ,  $1/r^4$ ,  $1/r^6$ , and  $1/r^{12}$ , respectively [for review see Fersht (1985)]. Thus, when the side chains at sites X and Y are remote to one another and assuming no large structural perturbations, the  $\Delta G_1$  term should be negligible and eq 1 thus simplifies to

$$\Delta\Delta G_{px,y} \approx \Delta\Delta G_m + \Delta\Delta G_{\bar{m}} \quad (2)$$

This situation, here referred to as simple additivity, is generally observed except where side chains are close to each other or when one or both of the mutants change the rate-limiting step or reaction mechanism. These principles are well illustrated from data of additive mutational effects on transition-state stabilization energies.



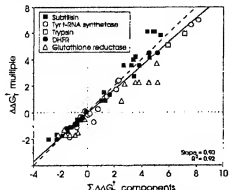


FIGURE 1: Plot of the changes in transition-state stabilization energies for the multiple mutant versus the sum for the component mutants. Data are taken from Table I and represent mutants from subtilisin (■), tyrosyl-tRNA synthetase (○), trypsin (●), DHFR (△), and glutathione reductase (▲), where mutant or wild-type side chains should not contact one another. The dashed line has a slope of 1, and the solid line is a best fit to all the data.

Changes in transition-state stabilization energy ( $\Delta\Delta G_{\ddagger}^*$ ) caused by a mutation can be calculated from eq 3 (Wilkinson et al., 1983), in which  $R$  is the gas constant,  $T$  is the absolute

$$\Delta\Delta G_{\ddagger}^* = -RT \ln \frac{(k_{cat}/K_M)_{mutant}}{(k_{cat}/K_M)_{wild-type}} \quad (3)$$

temperature,  $k_{cat}$  is the turnover number, and  $K_M$  is the Michaelis constant for the mutant and wild-type enzyme against a fixed substrate.  $\Delta\Delta G_{\ddagger}^*$  represents the change in free energy to reach the transition-state complex ( $E-S^*$ ) from the free enzyme and substrate ( $E + S$ ).

To analyze the proposition that the interaction energy term,  $\Delta G_{TQY}^*$ , is relatively small when the sites of mutation (X and Y) are remote to one another,  $\Delta\Delta G_{\ddagger}^*$  values were collected from the literature where side-chain substitutions in the multiple mutant are beyond the van der Waals contact ( $>4 \text{ \AA}$  distant) from each other (Table I). There are at least 25 examples distributed across five different enzymes where  $\Delta\Delta G_{\ddagger}^*$  values can be calculated for the individual and multiple mutants assayed in at least two different ways. Among these are examples where electrostatic interactions, hydrogen bonding, and steric and hydrophobic effects have been altered separately or in combination with others. The X-ray structures of the wild-type proteins show that the wild-type side chains are not in contact. Modeling suggests the mutant side chains are beyond possible van der Waals contact unless the mutant side chains were to cause significant changes in the overall protein structure. Such large changes are rarely observed in structures of site-specific mutant proteins (Katz & Kossiakoff, 1986; Alber et al., 1987; Howell et al., 1986; Wilde et al., 1988) or even highly variant natural proteins (Chothia & Lesk, 1986).

A collective plot of the sum of the  $\Delta\Delta G_{\ddagger}^*$  values for the component mutants versus the corresponding multiple mutant (Table I) gives a remarkably strong correlation ( $R^2 = 0.92$ ) with a slope near unity (Figure 1). The simplest interpretation is that the interaction term,  $\Delta G_{TQY}^*$ , is small compared to the overall effects on  $\Delta\Delta G_{TQY}^*$ . It is formally possible that there are large and compensating effects between side chains X and Y that systematically lead to small net values for  $\Delta G_{TQY}^*$ .

There are some notable exceptions that weaken the correlation within the data set (Table I). In particular, combining the R204L mutation in *Escherichia coli* glutathione reductase gives a less than additive effect, especially when combined with

another mutant, R198M (Scrutton et al., 1990). These basic residues are not in direct contact, but both side chains form a salt bridge with the 2'-phosphate group of NADPH. Indeed, the largest discrepancies are when these mutants are assayed with NADPH as compared to NADH. Similarly, the sum of the  $\Delta\Delta G_{\ddagger}^*$  values for two positively charged component mutants in subtilisin (D99K and E156K) overestimates the effect of the multiple mutant when assayed with an Arg but not with a Phe substrate (Russell & Fersht, 1987). Such discrepancies are not too surprising because charge-charge interactions fall off as  $1/r$  and can exhibit long-range effects in proteins [for example, see Russell and Fersht (1988)]. The physical basis for other large discrepancies not involving electrostatic substitutions is less clear but may involve unexpected large structural changes or changes in enzyme mechanism (see below).

These additivity tests are not particularly dominated by one of the single mutants in the sum. The average contribution ( $\pm SE$ ) for the most dominant mutant in each sum calculated from the 69 additivity tests given in Table I is only 68% ( $\pm 13\%$ ) of the total sum (theoretical is  $\sim 50\%$ ). Furthermore, the plot in Figure 1 is not analogous to graphs of correlated variables, where  $A$  is plotted versus the sum of  $A + B$ , because in Figure 1 the values on the  $y$ -axis are determined independently from those on the  $x$ -axis.

#### COMPLEX ADDITIVITY IN TRANSITION-STATE STABILIZATION—WHEN $\Delta G_{TQY}^* \approx 0$

(A) *Change in Interaction Energy between Sites X and Y.* Where residues X and Y are close enough to contact, it is more likely that the  $\Delta G_{TQY}^*$  term will be significant. There are 11 examples collectively from tyrosyl-tRNA synthetase and subtilisin that fit this category (Table II).

A series of mutants in tyrosyl-tRNA synthetase at positions 48 and 51 (Carter et al., 1984; Lowe et al., 1985) show complex additivity (Table II). His48 and Thr51 in the wild-type structure are next to each other on adjacent turns of an  $\alpha$ -helix. His48 hydrogen bonds to the ribose ring oxygen of ATP while Thr51 can make van der Waals contact with ATP. The T51P mutation increases the catalytic efficiency of the enzyme in some assays by more than  $-2 \text{ kcal/mol}$  (Wilkinson et al., 1984). However, when this mutation is combined with mutations at position 48, the effects are not simply additive. An X-ray structure of the T51P mutant indicates there are no structural changes in the  $\alpha$ -helix (Brown et al., 1987). Instead, it is suggested that the T51P mutant is improved over wild type because the wild-type enzyme contains a bound water in the vicinity of Thr51 that disfavors substrate binding. Blow and co-workers (Brown et al., 1987) argue that the change in solvent structure propagated to position 48 may account for the complex additivity. In the previous section, the double mutant (H48G, T51A) exhibited nearly simple additivity (Table I). Presumably, the smaller and less hydrophobic alanine substitution at position 51 should not introduce as large a change in solvent structure as the pyrrolidine ring of proline.

In the case of subtilisin (Table II), Glu156 is near the top of the P1 binding crevice while Gly166 is at the bottom. In the wild-type enzyme these sites do not make direct van der Waals contact, but large side chains substituted at position 166 can be modeled to contact the residue at position 156. In fact, X-ray structural analysis shows that an Asn side chain at position 166 makes a good hydrogen bond with Glu156 (Bott et al., 1987). Moreover, all of the substitutions are polar or charged, the energetics of which are expected to be the most long range. Thus, the mutant side chains alter substantially the intramolecular interactions between positions 156 and 166.

Table 1: Comparison of Sums of  $\Delta\Delta G_T^*$  from Component Mutants vs the Multiple Mutant Where the Mutant or Wild-Type Side Chains Do Not Contact One Another

$\Delta\Delta G_T^*$				$\Delta\Delta G_T^*$				
assay	component mutants	sum	multiple mutant	assay	component mutants	sum	multiple mutant	
Tyrosyl-tRNA Synthetase								
	C35G + H48G <sup>a</sup>				D99K + E156K			
ATP/PP <sub>i</sub>	+1.20 +1.04	+2.24	+2.30	R	+1.29 +2.12	+3.41	+2.74	
ATP/tRNA	+1.05 +1.13	+2.18	+1.68	F	+0.13 +1.49	-0.36	-0.42	
Tyr/PP <sub>i</sub>	+1.14 +1.12	+2.26	+2.32		E156S,			
Tyr/tRNA	+0.32 +1.12	+1.45	+1.20		G166A + G169A, Y217L <sup>b</sup>			
	C35G + T51P							
ATP/PP <sub>i</sub>	+1.20 -1.91	-0.71	-1.14	F	-0.40 -1.46	-1.86	-1.76	
ATP/tRNA	+1.05 -2.35	-1.30	-1.88	Y	+0.94 -1.03	-0.09	+0.02	
Tyr/PP <sub>i</sub>	+1.14 -1.14	+0.50	-0.74					
Tyr/tRNA	+0.32 +0.50	+0.82	+0.21					
	C35G + T51C <sup>c</sup>							
ATP/tRNA	+1.05 -0.93	+0.12	-0.22	F	-0.40 +4.96	+4.56	+4.11	
ATP/Tyr	+1.14 -0.91	+0.23	-0.13	Y	+0.94 +4.40	+5.34	+5.84	
	H48N + T51A <sup>c</sup>							
ATP/PP <sub>i</sub>	+0.26 -0.38	-0.12	+0.04	F	-1.46 +4.96	+3.50	+4.21	
ATP/tRNA	-0.13 -0.32	-0.45	-0.37	Y	-1.03 +4.40	+3.37	+3.96	
	T40A + H45Q <sup>c</sup>							
Tyr/Tyr	+5.02 +3.15	+8.17	+6.95					
ATP/Tyr	+5.13 +2.44	+7.57	+6.67					
Rat Trypsin								
K	G216A + G226A <sup>c</sup>	+5.88	+5.07	F	+4.21 -0.40	+3.81	+3.53	
R	+2.75 +3.13	+5.88	+5.07	Y	+1.26 +0.94	+4.90	+6.07	
	+2.19 +4.91	+7.10	+5.90		S24C, E156S, H64A, + G169A, G166A, Y217L			
Dihydrofolate Reductase ( $\Delta\Delta G_{\text{reductase}}$ )								
H <sub>2</sub> F	F31V + L54G <sup>c</sup>			F	+4.11 -1.46	+2.65	+3.53	
MTX	+1.6 +2.9	+4.5	+4.5	Y	+5.84 -1.03	+4.81	+6.07	
	+2.2 +2.9	+5.1	+4.5		S24C, G166A, H64A, G169A, Y217L			
Subtilisin BPN'								
E	E156S + Y217L + G169A <sup>c</sup>			F	+4.96 -1.76	+3.20	+3.53	
Q	-1.43 -0.87	-0.62	-2.92	-2.06	Y	+4.40 +0.02	+4.38	+6.07
A	-0.60 -0.36	-0.32	-1.28	-1.14				
K	-0.15 -0.41	-0.27	-0.83	-0.92				
M	+1.70 -0.08	-0.30	+1.32	+0.87				
F	-0.86 -0.32	-0.39	-1.57	-1.41	NADH	-1.10 -0.62	-1.72	-1.32
Y	-0.61 -0.29	-0.66	-1.56	-1.17	NADPH	+0.08 +2.68	+2.76	+2.11
	E156S + Y217L					A179G + R204L		
E	-1.43 -0.87	-2.30	-1.67	NADH	-1.10 +0.41	-0.69	-1.54	
Q	-0.60 -0.36	-0.96	-0.96	NADPH	+0.08 +2.42	+2.50	+0.87	
A	-0.15 -0.41	-0.56	-0.53		R198M + R204L			
K	+1.70 -0.08	+1.62	+1.33	NADH	-0.62 +0.41	-0.21	-0.51	
M	-0.86 -0.32	-1.18	-1.11	NADPH	+2.68 +2.42	+5.10	+3.70	
F	-0.61 -0.29	-0.90	-0.84		A179G + R204L			
Y	-0.24 -0.12	-0.41	-0.77	NADH	-1.10 -0.51	-1.61	-1.72	
	E156S + G169A			NADPH	+0.08 +3.70	+3.78	+2.22	
E	Y217L + G169A <sup>c</sup>					R198M + A179G, R204L		
Q	-0.67 -0.62	-2.29	-2.06					
A	-0.96 -0.32	-1.28	-1.14	NADH	-0.62 -1.54	-2.16	-1.72	
K	-0.53 -0.27	-0.80	-0.92	NADPH	+2.68 +0.87	+3.55	+2.22	
M	+1.33 -0.30	+1.03	+0.87		R204L + A179G, R198M			
F	-1.11 -0.39	-1.50	-1.41					
Y	-0.84 -0.66	-1.50	-1.17	NADH	+0.41 +1.32	-0.91	-1.72	
	-0.32 -0.41	-0.73	-0.59	NADPH	+2.42 +2.11	+4.53	+2.22	
	D99S + E156S <sup>c</sup>					R179G + R198M + R204L		
R	+0.47 +0.77	+1.24	+1.52	NADH	-1.10 -0.62 +0.41	-1.31	-1.72	
F	0 -0.62	-0.62	-0.52	NADPH	+0.08 +2.68 +2.42	+5.18	+2.22	

\* Carter et al. (1984). The assays refer to measurements of ATP-dependent pyrophosphate exchange (ATP/PP<sub>i</sub>) or tRNA charging (ATP/tRNA) under saturating conditions for tyrosine and vice versa for Tyr/PP<sub>i</sub> exchange and Tyr/tRNA charging. <sup>a</sup> Lowe et al. (1985). The ATP/Tyr activation assay refers to formation of tyrosyl adenylate under saturating concentrations of tyrosine. <sup>b</sup> Jones et al. (1986). <sup>c</sup> Leatherbarrow et al. (1986). The ATP/Tyr and Tyr/Tyr activation assays refer to formation of tyrosyl adenylate under pre-steady-state conditions, and  $k_{on}/k_{off}$  is calculated from  $k_1/k_2$  for tyrosine and ATP, respectively. <sup>d</sup> Crail et al. (1985). The substrate was D-Val-Leu-(X)-aminofluorocoumarin where the P1 residue (X) is either Lys (K) or Arg (R). <sup>e</sup> Mayer et al. (1986). The ligand was either dihydrofolate (H<sub>2</sub>F) or methotrexate (MTX). <sup>f</sup> Wells et al. (1987a). The substrate was succinyl-L-Ala-L-Gly-L-Ala-L-Pro-L-(X)-succinamide where the P1 (X) residue (Schechter & Berger, 1937) was either Glu (E), Gln (Q), Ala (A), Lys (K), Asp (D), Phe (F), or Tyr (Y). <sup>g</sup> Kroll and Ferst (1987). The substrate was benzyl-L-Val-Gly-L-Arg-p-nitroanilide (R) or succinyl-L-Ala-L-Ala-L-Pro-L-Phe-p-nitroanilide (F). <sup>h</sup> Carter et al. (1989). The substrate was succinyl-L-Pho-L-Ala-L-His-L-(X)-p-nitroanilide where X was either Phe (F) or Tyr (Y). <sup>i</sup> Scruton et al. (1990). The assay followed the reduction of oxidized glutathione by NADH or NADPH.

Table II: Comparison of Sums of  $\Delta\Delta G_f^\circ$  from Component Mutants vs the Multiple Mutant Where the Mutant Side Chains Can Contact One Another

assay*	$\Delta\Delta G_f^\circ$		
	component mutants	sum	multiple mutant
Tyrasyl-tRNA Synthetase			
H48G + T51P <sup>a</sup>	+1.06	-1.91	-0.87
ATP/PP <sub>i</sub>	+1.13	-2.35	-1.22
Tyr/PP <sub>i</sub>	+1.12	-0.64	+0.48
Tyr/tRNA	+1.12	+0.50	+1.63
ATP/Tyr <sup>b</sup>	+0.95	-1.99	-1.04
ATP/ATP	+1.07	-0.38	+0.69
H48N + T51P <sup>a</sup>			
ATP/Tyr	+0.18	-1.99	-1.81
Tyr/Tyr	+0.36	-0.38	-0.02
ATP/tRNA	-0.02	-2.23	-2.25
N48G + T51P <sup>a</sup>			
ATP/Tyr	+0.31	-0.94	-0.57
Tyr/Tyr	+0.41	-1.00	-0.59
ATP/tRNA	+1.26	-1.05	+0.21
Q48C + T51P <sup>a</sup>			
ATP/Tyr	-1.31	-1.09	-2.40
Tyr/Tyr	-2.05	-1.65	-3.70
ATP/tRNA	-1.87	-1.85	-3.72
H48Q + T51P <sup>a</sup>			
ATP/Tyr	+2.26	-1.99	+0.27
Tyr/Tyr	+3.13	-0.38	+2.75
ATP/tRNA	+3.11	-2.23	+0.88
Subtilisin BPN'			
E156Q + G166D <sup>a</sup>			
Q	-1.04	+1.27	+0.23
M	-0.45	+1.83	+1.38
K	+2.15	+0.53	+2.68
E156S + G166D			
Q	-0.59	+1.27	+0.68
M	-0.85	+1.83	+0.98
K	+1.68	+0.53	+2.22
E156Q + G166N			
E	-1.71	-1.04	-1.82
Q	-0.94	-0.14	-0.90
M	-0.45	+0.18	-0.27
K	+2.15	+0.48	+2.73
E156S + G166N			
E	-1.44	-0.11	-1.55
Q	-0.59	+0.14	-0.45
M	-0.85	+0.18	-0.67
K	+1.68	+0.48	+2.16
E156S + G166K			
E	-1.44	-3.49	-4.93
Q	-0.59	-1.03	-1.62
M	-0.85	-1.37	-2.22
K	+1.68	+0.51	+2.19
E156Q + G166K			
E	-1.71	-3.49	-5.20
Q	-1.04	-1.03	-2.07
M	-0.45	-1.37	-1.82
K	+2.15	+0.51	+2.66

\*See Table I for description assays. <sup>a</sup>Lowe et al. (1985). <sup>b</sup>Carter et al. (1984). <sup>c</sup>Wells et al. (1987b).

In these six examples there are large and systematic discrepancies between the sum of the  $\Delta\Delta G_f^\circ$  values for the single mutants and those of the corresponding double mutant (Wells et al., 1987b). In almost all cases, the sum of the  $\Delta\Delta G_f^\circ$  values for the single mutants is much greater than the value for the multiple mutant. Nonetheless, the  $\Delta\Delta G_f^\circ$  value predicted from the sum of the single mutants does have the same sign as that for the double mutant, so that the single mutants predict qualitatively the effect on the multiple mutant.

A plot (Figure 2) of the collective data set from Table II is in contrast to that seen in Figure 1. The  $\Delta\Delta G_f^\circ$  values for the multiple mutants correlate more poorly with the sum of

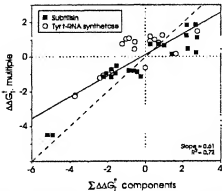


FIGURE 2: Data are taken from Table II for mutants of subtilisin (■) or tyrosyl-tRNA synthetase (○) where mutant or wild-type side chains can contact each other. The dashed line represents a theoretical line of unity slope, and the solid line represents the best fit.

the component single mutants ( $R^2 = 0.72$ ). Moreover, the slope of the line (0.61) is much below unity. This indicates that the function of one residue is compromised by mutation of another. Of the 40 additivity examples, the average contribution of the most dominant single mutant to the sum of the  $\Delta\Delta G_f^\circ$  values is 71% ( $\pm 13\%$ ) of the total. Thus (as in Figure 1), both single mutants can contribute substantially to free energy changes measured in the multiple mutant. However, this data set is derived from mutations at only two different sites on two different proteins.

In summary, complex additivity can be observed when mutations at sites X and Y change the intramolecular interaction energy between sites. This can be mediated by direct steric, electrostatic, hydrogen-bonding, or hydrophobic interactions or indirectly through large structural changes in the protein, solvent shell, or electrostatic interactions. Complex additivity is most likely to occur where the sites of mutation are very close together and larger or chemically divergent side chains are introduced.

**B. Mutations at Sites X or Y Change the Enzyme Mechanism or Rate-Limiting Step.** If the catalytic functions of two or more residues are interdependent, then a mutation of one residue can affect the functioning of the other(s). This form of complex additivity is well illustrated for mutations in the catalytic triad and oxyanion binding site of subtilisin (Carter & Wells, 1988, 1990). In the catalytic mechanism of subtilisin (Figure 3), the rate-limiting step in amide bond hydrolysis is transfer of the proton from Ser221 to His64 with nucleophilic attack upon the scissile carbonyl carbon. This is accompanied by electrostatic stabilization of the protonated imidazole by Asp32 and hydrogen bonding to the oxyanion by the side chain of Asn155 and the main-chain amide of Ser221. Mutational analysis shows that once the catalytic Ser221 is mutated to Ala (S221A), additional mutations in the triad or oxyanion binding site cause no further loss in catalytic efficiency (Table III).

The S221A enzyme retains a catalytic activity that is still 10<sup>7</sup> times above the solution hydrolysis rate (Carter & Wells, 1988). It is proposed that this residual activity is derived from remaining transition-state binding contacts outside of the catalytic triad coupled with solvent attack upon the carbonyl carbon from the face opposite position 221 (Carter & Wells, 1990). This proposal is based on a model showing that there is no room for a water molecule near Ala221 once the substrate is bound. Furthermore, conversion of Asn155 to Gly enhances the activity of the S221A mutant by ~1.2 kcal/mol (Table III).

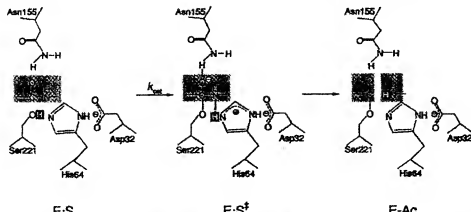


FIGURE 3: Schematic diagram of the mechanism of subtilisin showing the rate-limiting acylation step for hydrolysis of peptide bonds. Reproduced with permission from Carter and Wells (1988). Copyright 1988 Macmillan.

Table III: Comparison of  $\Delta\Delta G_{\text{cat}}^{\ddagger}$  from Component Mutants vs the  $\Delta\Delta G_{\text{cat}}^{\ddagger}$  for Multiple Mutants in the Catalytic Triad and Oxyanion Binding Site of Subtilisin BPN'

component mutants	sum	multiple mutant
S221A + H64A <sup>b</sup>	+8.84	+8.83
+8.93      +8.84	+17.76	+8.83
S221A + D32A	+6.52	+8.86
+8.93      +6.52	+15.45	+8.86
H64A + D32A	+6.52	+7.48
+8.84      +6.52	+15.36	+7.48
S221A + H64A + D32A	+6.52	+7.48
+8.93      +8.84      +6.52	+24.29	+8.65
S221A + H64A	+6.52	+8.65
+8.93      +7.48	+16.40	+8.65
H64A + S221A	+6.52	+8.65
+8.84      +6.52	+17.70	+8.65
D32A + S221A	+6.52	+8.65
+6.52      +8.83	+15.35	+8.65
S221A + N155G <sup>c</sup>	+3.08	+7.70
+8.93      +3.08	+12.01	+7.70

<sup>a</sup>All enzymes were assayed with the substrate succinyl-L-Ala-L-Ala-L-Pro-L-Phe-p-nitroanilide. <sup>b</sup>Carter and Wells (1988). <sup>c</sup>Carter and Wells (1990).

This is consistent with the opposite-face solvent attack mechanism of S221A, because the oxyanion (Figure 3) would develop away from Asn155 and the N155G mutation improves solvent accessibility to the scissile carbonyl carbon.

Complex additivity is also seen for subtilisin mutated at positions 64 and 32. The double (H64A,D32A) and corresponding single mutants show a linear dependence upon hydroxide ion concentration (between pH 8 and 10) that may reflect hydroxide assistance in the deprotonation of the O<sub>γ</sub> of Ser221 (Carter & Wells, 1988). Thus, once His64 is converted to Ala, Asp32 is a liability, presumably by electrostatic repulsion of hydroxide ion. [Note the -1.3 kcal/mol improvement in  $\Delta\Delta G_{\text{cat}}^{\ddagger}$  for the double mutant (H64A,D32A) compared to H64A alone; Table III.]

In summary, if an enzyme mechanism relies upon cooperative interaction between two or more residues, then multiple mutations within this subset can result in large values for  $\Delta\Delta G_{\text{cat}}^{\ddagger}$ . In fact, if the mechanism is changed substantially, residues that were a catalytic asset can become a liability. Simple additivity can also break down when one or more of the mutations cause a change in the rate-limiting step. In an extreme case, one may have a number of mutants in an enzyme that enhance the activity, but the cumulative enhancement of

activity could not go beyond the diffusion-controlled limit (Allery & Knowles, 1976).

#### ADDITIONAL EFFECTS ON SUBSTRATE BINDING

The analysis above considered changes in binding free energies between the free enzyme and substrate ( $E + S$ ) to yield the bound transition-state complex ( $E \cdot S^{\ddagger}$ ). The steady-state kinetic analysis for subtilisin and tyrosyl-tRNA synthetase is such that the  $K_m$  values approximate the enzyme-substrate dissociation constant  $K_d$ . Additivity analysis based on calculations of  $\Delta\Delta G_{\text{binding}}$  (from  $K_m$  values) or  $\Delta\Delta G_{\text{on}}$  (from  $k_{\text{on}}$  values) yields qualitatively the same results (not shown) as shown in Tables I and II and Figures 1 and 2. Thus, deviations from simple additivity are not systematically found in either the energetics to form the  $E \cdot S$  complex or those to reach  $E \cdot S^{\ddagger}$ .

#### ADDITIONAL EFFECTS ON PROTEIN-PROTEIN INTERACTIONS

The first clear examples of additive binding effects caused by amino acid replacements in proteins were reported by Laskowski et al. (1983) and reviewed by others (Ackers & Smith, 1985; Horowitz & Rigbi, 1985). One hundred natural variants of a proteinase inhibitor, the ovoacacid third domain, have been isolated and sequenced from the eggs of different bird species (Empie & Laskowski, 1982; Laskowski et al., 1987). This is a nested set of proteins because for any one of these avian inhibitors there is a close relative containing only one or a few amino acid substitutions. Moreover, the association constants ( $K_a$ ) of these inhibitors with a variety of serine proteinases vary over an enormous range (10<sup>4</sup>-fold). Laskowski et al. (1983, 1989) have shown that the effect of a given residue replacement on  $K_a$  is about the same irrespective of the inhibitor scaffold the replacement is made in.

In addition to ovoacacid, four additivity examples have been constructed from natural variants at the subunit interface of tetrameric hemoglobin (Ackers & Smith, 1985). Three additivity examples have been analyzed for interactions of hGH with its receptor (B. C. Cunningham and J. A. Wells, unpublished results) and one example for association of synthetic variants of the RNase S peptide with RNase S protein (Mitchison & Baldwin, 1986). The entirety of this data set is not tabulated because much on the ovoacacid inhibitors and hGH is unpublished. Nonetheless, these researchers were kind enough to provide their data formatted so it could be plotted collectively in Figure 4. These data consist of 91 additivity examples (80 in ovoacacid alone), representing 22 multiple mutants across four different proteins, and span a wide range of change in binding free energy (-10 to +7

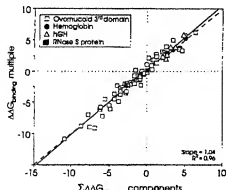


FIGURE 4: Plot showing the sum of changes in free energies of binding at protein-protein interfaces for component mutants versus the corresponding multiple mutant. Data represent interactions between ovomucoid third domain and various serine proteases ( $\square$ ) (R. Wynn and M. Laskowski, personal communication), regulatory interface of  $\alpha_2$ -globin ( $\bullet$ ) (Ackers & Smith, 1985), HbH and its receptor (stippled  $\Delta$ ) (B. Cunningham and J. Wells, personal communication), and RNase S peptide and S protein ( $\blacksquare$ ) (Mitchison & Baldwin, 1986). The dashed line represents a line of unity slope, and the solid line is the best fit.

kcal/mol). The plot shows a very strong linear correlation ( $R^2 = 0.96$ ) with a slope near unity. Although the data for the ovomucoid were not sorted to evaluate changes at intramolecular contact sites, most are not expected to be in contact, and all of the other examples represent noncontact sites. Thus, the large data base derived from natural variants of ovomucoid third domain, as well as a smaller number of examples from several other proteins, indicates that multiple mutations at protein-protein interfaces commonly produce simple additive effects.

#### ADDITIONAL EFFECTS IN DNA-PROTEIN INTERACTIONS

One of the clear advantages in analyzing DNA-protein interactions is the ability to apply powerful selections that make analysis by random mutational studies feasible. Additivity in DNA-protein interactions was first demonstrated by revision analysis of  $\lambda$  repressor (Nelson & Sauer, 1985). A mutation that decreased the binding affinity for the  $\lambda$  operator site (K4Q) was reverted by mutations at several second sites (E34K, G48S, and E83K). When these second-site revertants were introduced into wild-type  $\lambda$  repressor, they caused increases in affinity similar to those observed in the first-site suppressor mutant (K4Q).

Functional independence for mutations at DNA-protein contacts has been demonstrated by additive effects for mutants of CAP (catabolite gene activator protein) and its operator sequence (Ebright et al., 1987) as well as *lac* repressor and its corresponding operator sequence (Ebright, 1986). Simple additivity of mutational effects in the operator sequences for Cro repressor (Takeda et al., 1989) and  $\lambda$  repressor (Sarai & Takeda, 1989) has been most systematically demonstrated. Simple additivity has also been reported for multiple mutations in the *lac* repressor (Lehming et al., 1990). In fact, simple additivity is so predictable in DNA-protein interactions that the observation of complex additivity has been used to predict specific DNA-protein contacts in the *lac* repressor-operator complex (Ebright, 1986).

#### ADDITIONAL EFFECTS ON PROTEIN STABILITY

The first systematic analysis of additive effects of site-specific mutations on protein stability was reported by Shortle and Meeker (1986). Five multiple mutants in staphylococcal

Table IV: Comparison of Sums of  $\Delta\Delta G_{\text{addition}}$  from Component Mutants vs the Multiple Mutant

assay	component mutants	$\Delta\Delta G_{\text{addition}}$	
		sum	multiple mutant
Staphylococcal Nuclease			
GuHCl	V66I + G79S*	-2.8	-3.3
urea	+0.2 -2.9	-2.7	-3.6
GuHCl	V66I + G88V	-1.0	-2.1
urea	+0.2 -0.9	-0.7	-1.4
GuHCl	I18M + A59T	-2.7	-2.8
urea	-0.6 -2.7	-3.3	-3.6
GuHCl	I18M + A90S	-2.9	-2.8
urea	-0.7 -2.9	-3.6	-3.4
N-Terminal Domain of $\lambda$ Repressor			
GuHCl	G46A + G48A*	+0.9	+1.1
thermal melt	+0.7	+1.6	+1.1
T4 Lysozyme			
GuHCl	I3C + C54V*	-0.7	-0.4
thermal melt	+1.2 -0.7	+0.5	+0.4
GuHCl	I3C + C54T	-0.7	-0.4
thermal melt	+1.2 +0.3	+1.5	+1.5
GuHCl	I3C + C54T + R96H	-2.8	-2.5
thermal melt	+1.2 +0.3 -2.8	-1.3	-2.5
GuHCl	I3C, C54T + R96H	-2.8	-2.5
thermal melt	+1.5 -2.8	-1.3	-2.5
GuHCl	I3C + C54T + A146T	-1.5	-0.5
thermal melt	+1.2 +0.3 -1.5	0	-0.5
GuHCl	I3C, C54T + A146T	-1.5	-0.5
thermal melt	+1.5 -1.5	0	-0.5
Bacteriophage f1 Gene V			
GuHCl	V35I + I47V*	-2.4	-2.9
GuHCl	-0.4	-2.8	-2.9
Kringle-2 of tPA			
GuHCl	H64Y + R68G*	+0.7	+3.6
GuHCl	+2.9	+3.6	+3.4
Turkey Ovomucoid Third Domain			
GuHCl	G32A + N28S*	-0.5	-0.2
GuHCl	+0.8 -0.5	+0.3	+0.2
GuHCl	Y20H + N45-CHO	-0.8	-0.5
GuHCl	+0.3	-0.5	-0.5
$\alpha$ Subunit of <i>E. coli</i> Trp Synthetase			
GuHCl	Y175C + G211E*	+0.3	+0.2
GuHCl	-0.1	+0.2	-1.3

\*Shortle and Meeker (1986). \*Hecht et al. (1986). \*Wetzell et al. (1988). \*Sandberg and Terwilliger (1989). \*R. Kelley, personal communication. \*Oleksiw and Laskowski (1990). N45-CHO refers to a glycosylation of Asn45. \*Hurle et al. (1986).

nuclease were constructed from a group of random single mutants that were screened initially for their ability to affect the stability of the enzyme *in vivo*. The component mutants do not make direct contact with each other in the multiple mutants. Generally, these variants exhibit nearly additive effects except for the double mutant V66I,G88V (Table IV). In addition to those of staphylococcal nuclease, additive effects on the  $\Delta\Delta G_{\text{addition}}$  (assayed by reversible denaturation) have also been determined for the N-terminal domain of  $\lambda$  repressor (one example, Hecht et al., 1986), the  $\alpha$ -subunit of *E. coli* Trp synthetase (one example; Hurle et al., 1986), T4 lysozyme (six examples; Wetzell et al., 1988), the gene V product of bacteriophage f1 (one example; Sandberg & Terwilliger, 1989),

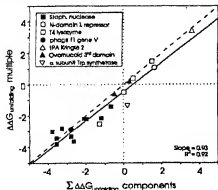


FIGURE 5: Plot showing sum of changes in free energy of unfolding of component mutants and resulting multiple mutant. Data are taken from Table IV and represent staphylococcal nuclease (■), N-terminal domain of a repressor (○), T4 lysozyme (○), bacteriophage f1 gene V product (△), Kringle 2 domain of tissue plasminogen activator (▲), ovomucoid third domain (△), and the  $\alpha$ -subunit of Trp synthetase (○). The dashed line represents a theoretical line of unity slope, and the solid line represents the best fit.

natural variants of ovomucoid third domain (two examples; Otlewski & Laskowski, 1990), and the Kringle-2 domain of human tissue plasminogen activator (t-PA) (one example; R. Kelley, personal communication).

Collectively, this data set gives a high linear correlation ( $R^2 = 0.94$ ) and slope near unity (Figure 5). The generally simple additive behavior is somewhat surprising given the highly cooperative nature of protein folding. There are discrepancies in some of the additivity examples besides the staphylococcal nuclease mutant (V66L,G88V). For example, the 1.5 kcal/mol discrepancy for the Y175C,G271E double mutant in Trp synthetase (Table IV) is proposed to result from the fact that these residues are in direct contact (Hurlé et al., 1986). Furthermore, proximity effects may account for the large differences between the sum of the component mutants and the multiple mutants for the  $\alpha$ -helical double glycine mutant G46A,G48A in  $\lambda$  repressor (Hecht et al., 1986), and when combining R96H with the C3-C97 disulfide mutant in T4 lysozyme (Wetzell et al., 1988). In contrast, an exchange of two side chains that contact one another (V35I and I47V) in the hydrophobic core of the gene V product of f1 phage produced simple additive effects (Sandberg & Terwilliger, 1989; Table IV). It should be noted that this data base exhibiting simple additivity may be biased for single mutants that stably fold, because severely unstable proteins are more difficult to express.

By analogy to transition-state binding effects, one can certainly imagine instances where the stabilizing effects of mutations should reach a plateau. For example, denaturation at high temperatures can become controlled by a chemical step such as deamidation (Ahern et al., 1987), so that additional mutants that stabilize the folded form of the protein may be irrelevant. Another obvious example where complex additivity can be observed in protein stability is the stabilizing effect of disulfide bonds and noncovalent intramolecular contacts that require interactions between two or more residues. In these cases, the stabilizing interaction between two side chains can be broken with only one mutation.

#### APPLICATIONS OF ADDITIVITY IN RATIONAL PROTEIN DESIGN

A strategy of additive mutagenesis, where a series of single mutants each making a small improvement in function are

combined, is one of the most powerful tools in designing functional properties in proteins. This approach has been remarkably successful in stabilizing proteins to irreversible inactivation, such as  $\lambda$  repressor (Hecht et al., 1986), subtilisin (Bryan et al., 1987; Cunningham & Wells, 1987; Pantoliano et al., 1989), kanamycin nucleotidyltransferase (Liao et al., 1986; Matsumura, 1986), neutral protease (Imanaka et al., 1986), and T4 lysozyme (Wetzell et al., 1988; Matsumura et al., 1989). This strategy has been applied to enhancing the catalytic efficiency of a weakly active variant of subtilisin (Carter et al., 1989), engineering the substrate specificity of subtilisin (Wells et al., 1987a,b; Russell & Fersht, 1987) and the coenzyme specificity of glutathione reductase (Scrutton et al., 1990), designing protease inhibitors with exquisite protease specificity (Laskowski et al., 1989), and recruiting human prolactin to bind to the hGH receptor (Cunningham et al., 1990). In addition, additivity principles have been used to engineer the pH profile of subtilisin (Russell & Fersht, 1987) and design the affinity and specificity of  $\lambda$  repressor (Neison & Sauer, 1985).

For this approach to work does not require that all the component mutants act in a simply additive manner but just that their effects accumulate. For example, despite the complex additivity of effects in the catalytic triad of subtilisin, there are mutagenic pathways that are energetically cumulative for installing the triad (Carter & Wells, 1988; Wells et al., 1987c). Starting with the triple mutant S221A,H64A,D32A, there is a progressive enhancement for installing Ser221 (-1.1 kcal/mol), then His64 (-1.0 kcal/mol), and finally Asp32 (-6.5 kcal/mol). Another cumulative pathway of Ser221, then Asp32, and finally His64 is possible if the Ser221,Asp32 intermediate were to use HisP2 substrates (Carter & Wells, 1987). Elaborating such cumulative pathways important for understanding how a catalytic apparatus may have evolved and is practically useful for considering how to install such catalytic machinery into weakly active catalytic antibodies.

#### CONCLUSIONS

In the majority of cases, combination of mutations that affect substrate or transition-state binding, protein-protein interactions, DNA-protein recognition, or protein stability exhibits simple additivity. Simple additivity is commonly observed for distant mutations at rigid molecular interfaces such as in protein-protein and DNA-protein interactions, where the mutations are unlikely to alter grossly the structure or mode of binding.

Large deviations from simple additivity can occur when the sites of mutations strongly interact with one another (by making direct contact or indirectly through electrostatic interactions or large structural perturbations) and/or when both sites function cooperatively (as for the catalytic triad and oxyanion binding site of subtilisin). Changes at sites that can contact each other do not always lead to complex additivity; this may reflect relatively weak interactions between the two sites or indicate that the interactions are compensatory and appear to be weak.

It is important to point out the magnitude of errors in predicting the free energy effect in the multiple mutant from the component single mutants. Generally, for those cases exhibiting simple additivity (Figures 1, 4, and 5), the discrepancy in free energy between the sums of the components and multiple mutants is about  $\pm 25\%$ . Part of this is the result of compounding errors when summing the single mutants, and the rest is presumably due to weak interaction terms. Nonetheless, this means that if the total free energy change is about 3 kcal/mol, the change in the equilibrium constant

(related by  $K_{t,y}/K_{w} = 10^{3/RT} = 155$ ) will often be off by a factor of 4. Thus, while the free energy effects accumulate, significant deviations will occur in predicting the final equilibrium constants when component mutants contribute a large free energy term.

Simple additivity reflects the modularity of component amino acids in protein function. This results from the fact that the perturbations in energetics and structure resulting from most mutations are highly localized. In the past six years, an additive mutagenesis strategy has been extremely effective in engineering proteins—of course, nature has been using this strategy much longer.

#### ACKNOWLEDGMENTS

I am grateful to Dr. Michael Laskowski and Rich Wynn for providing their data prior to publication on ovomucoid third domain and similarly to Brian Cunningham, Paul Carter, and Robert Kelley for making available their unpublished data. I am indebted for useful discussions with Drs. Michael Laskowski, Paul Carter, Jack Kirsch, and Tony Kossiakoff and many of my colleagues at Genentech and to Drs. Richard Ebright and William Jencks and those above for critical reading of the manuscript.

**Registry No.** RNase, 9001-99-4; tyrosyl-tRNA synthetase, 9023-45-4; trypsin, 9002-07-7; dihydrofolate reductase, 9002-03-3; subtilisin, BPN' 9014-01-1; glutathione reductase, 9001-48-3; staphylococcal nuclease, 9013-53-0; hexamerin, 9001-63-2; plaminogen activator, 105913-11-9; tryptophan synthetase, 9014-52-2.

#### REFERENCES

- Ackers, G. K., & Smith, F. R. (1985) *Annu. Rev. Biochem.* **54**, 597-629.
- Ahern, T. J., Casal, J. I., Petisko, G. A., & Klisbov, A. M. (1987) *Proc. Natl. Acad. Sci. U.S.A.* **84**, 675-679.
- Alber, T., Dao-pin, S., Wilson, K., Wozniak, J. A., Cook, S. P., & Matthews, B. W. (1987) *Nature* **330**, 41-46.
- Albery, W. J., & Knowles, J. R. (1976) *Biochemistry* **15**, 5631-5640.
- Ardelt, W., & Laskowski, M., Jr. (1990) *J. Mol. Biol.* (submitted for publication).
- Bott, R., Ultsch, M., Wells, J., Powers, D., Burdick, D., Struble, M., Burnier, J., Estell, D., Miller, J., Graycar, T., Adams, R., & Power, S. (1987) *ACS Symposium Series* **334** (LeBaron, H. M., Mumma, R. O., Honeycutt, R. C., & Deusing, J. H., Eds.) pp 139-147, American Chemical Society, Washington, DC.
- Brown, K. A., Brick, P., & Blow, D. M. (1987) *Nature* **326**, 416-418.
- Bryan, P. N., Rollence, M.-L., Pantoliano, M. W., Wood, J., Finzel, B. C., Gilliland, G. L., Howard, A. J., & Poulos, T. L. (1987) *Proteins: Struct., Funct., Genet.* **1**, 326-334.
- Carter, P., & Wells, J. A. (1987) *Science* **237**, 394.
- Carter, P., & Wells, J. A. (1988) *Nature* **332**, 564-568.
- Carter, P., & Wells, J. A. (1990) *Proteins: Struct., Funct., Genet.* (in press).
- Carter, P., Nilsson, B., Burnier, J. P., Burdick, D., & Wells, J. A. (1989) *Proteins: Struct., Funct., Genet.* **6**, 240-248.
- Carter, P. J., Winter, G., Wilkinson, A. J., & Fersht, A. R. (1984) *Cell* **38**, 835-840.
- Chothia, C., & Lesk, A. (1986) *EMBO J.* **5**, 823-826.
- Craik, C. S., Largman, C., Fletcher, T., Rocznak, S., Barr, P. J., Fletterick, R., & Rutter, W. J. (1985) *Science* **238**, 291-297.
- Cunningham, B. C., & Wells, J. A. (1987) *Protein Eng.* **1**, 319-325.
- Cunningham, B. C., Henner, D. J., & Wells, J. A. (1990) *Science* **247**, 1461-1465.
- Ebright, R. H. (1986) *Proc. Natl. Acad. Sci. U.S.A.* **83**, 303-307.
- Ebright, R. H., Kolb, A., Buc, H., Kunkel, T. A., Krakow, J. S., & Beckwith, J. (1987) *Proc. Natl. Acad. Sci. U.S.A.* **84**, 6083-6087.
- Empie, M. W., & Laskowski, M., Jr. (1982) *Biochemistry* **21**, 2274-2284.
- Fersht, A. (1985) in *Enzyme Structure and Mechanism*, 2nd ed., Chapters 3, 12, and 13, W. H. Freeman and Co., New York.
- Fersht, A. R. (1987) *Biochemistry* **26**, 8031-8037.
- Fersht, A. R., Wilkinson, A. J., Carter, P., & Winter, G. (1985) *Biochemistry* **24**, 5858-5861.
- Hecht, M. H., Sturtevant, J. M., & Sauer, R. T. (1986) *Proteins: Struct., Funct., Genet.* **1** 43-46.
- Horowitz, A., & Rigbi, M. (1985) *J. Theor. Biol.* **116**, 149-159.
- Howell, E. E., Villafranca, J. E., Warren, M. S., Oatley, S. J., & Kraut, J. (1986) *Science* **231**, 1123-1128.
- Hurle, M. R., Tweedy, N. B., & Matthews, C. R. (1986) *Biochemistry* **25**, 6356-6360.
- Imanaka, T., Shibasaki, M., & Takagi, M. (1986) *Nature* **324**, 695-697.
- Jencks, W. P. (1981) *Proc. Natl. Acad. Sci. U.S.A.* **78**, 4046-4050.
- Jones, M. D., Lowe, D. M., Borgford, T., & Fersht, A. R. (1986) *Biochemistry* **25**, 1887-1891.
- Katz, B. A., & Kossiakoff, A. (1986) *J. Biol. Chem.* **261**, 15480-15485.
- Laskowski, M., Jr., Tashiro, M., Empie, M. W., Park, S. J., Kato, I., Ardel, W., & Mieczorek, M. (1983) in *Protease Inhibitors: Medical and Biological Aspects* (Katunuma, N., Ed.) pp 55-68, Japan Scientific Societies Press, Tokyo, Japan.
- Laskowski, M., Jr., Kato, I., Ardel, W., Cook, J., Denton, A., Empie, M. W., Kohr, W. J., Park, S. J., Parks, K., Schatzley, B. L., Schoenberger, O. L., Tashiro, M., Vichot, G., Whatley, H. E., Wieczorek, A., & Wieczorek, M. (1987) *Biochemistry* **26**, 202-221.
- Laskowski, M., Jr., Park, S. J., Tashiro, M., & Wynn, R. (1989) in *Protein Recognition of Immobilized Ligands*, UCLA Symposia on Molecular and Cellular Biology (Hutchens, T. W., Ed.) Vol. 80, pp 149-160, A. R. Liiss, New York.
- Leatherbarrow, R. J., Fersht, A. R., & Winter, G. (1985) *Proc. Natl. Acad. Sci. U.S.A.* **82**, 7840-7844.
- Lehming, N., Sartorius, J., Kisters-Woike, B., von Wilcken-Bergmann, B., & Muller-Hill, B. (1990) *EMBO J.* **9**, 615-621.
- Liao, H., McKenzie, T., & Hageman, R. (1985) *Proc. Natl. Acad. Sci. U.S.A.* **82**, 576-580.
- Lowe, D. M., Fersht, A. R., Wilkinson, A. J., Carter, P., & Winter, G. (1985) *Biochemistry* **24**, 5106-5109.
- Matsuura, M., Yasumura, S., & Aiba, S. (1986) *Nature* **323**, 356-358.
- Matsuura, M., Signor, G., & Matthews, B. W. (1989) *Nature* **342**, 291-294.
- Matthews, B. W. (1987) *Biochemistry* **26**, 6885-6888.
- Mayer, R. J., Chen, J.-T., Taira, K., Fierke, C. A., & Benovic, S. J. (1986) *Proc. Natl. Acad. Sci. U.S.A.* **83**, 7718-7720.
- Mitchison, C., & Baldwin, R. L. (1986) *Proteins: Struct., Funct., Genet.* **1**, 23-33.

- Nelson, H. C. M., & Sauer, R. T. (1985) *Cell* 42, 549-558.
- Olewski, J., & Laskowski, M., Jr. (1990) (submitted for publication).
- Pantoliaco, M. W., Whittle, M., Wood, J. F., Dodd, S. W., Hardman, K. D., Rollence, M. L., & Bryan, P. N. (1989) *Biochemistry* 28, 7205-7213.
- Russell, A. J., & Fersht, A. R. (1987) *Nature* 328, 496-500.
- Sandberg, W. S., & Terwilliger, T. C. (1989) *Science* 245, 54-57.
- Sarai, A., & Takeda, Y. (1989) *Proc. Natl. Acad. Sci. U.S.A.* 86, 6513-6517.
- Schechter, I., & Berger, A. (1967) *Biochem. Biophys. Res. Commun.* 27, 157-162.
- Scrutton, N. S., Berry, A., & Perham, R. N. (1990) *Nature* 343, 38-43.
- Shortle, D., & Meeker, A. K. (1986) *Proteins: Struct., Funct., Genet.* 1, 81-89.
- Takeda, Y., Sarai, A., & Rivera, V. M. (1989) *Proc. Natl. Acad. Sci. U.S.A.* 86, 439-443.
- Wells, J. A., & Estell, D. A. (1988) *Trends Biochem. Sci.* 13, 291-297.
- Wells, J. A., Cunningham, B. C., Graycar, T. P., & Estell, D. A. (1987a) *Proc. Natl. Acad. Sci. U.S.A.* 84, 5167-5171.
- Wells, J. A., Powers, D. B., Bott, R. R., Graycar, T. P., & Estell, D. A. (1987b) *Proc. Natl. Acad. Sci. U.S.A.* 84, 1219-1223.
- Wells, J. A., Cunningham, B. C., Graycar, T. P., Estell, D. A., & Carter, P. (1987c) *Cold Spring Harbor Symp. Quant. Biol.* 52, 647-652.
- Wetzel, R., Perry, L. J., Baase, W. A., & Becktel, W. J. (1988) *Proc. Natl. Acad. Sci. U.S.A.* 85, 401-405.
- Wilde, J. A., Bolton, P. H., Dell'Acqua, M., Hibler, D. W., Pourmatabbed, T., & Gerlt, J. A. (1988) *Biochemistry* 27, 4127-4132.
- Wilkinson, A. J., Fersht, A. R., Blow, D. M., & Winter, G. (1983) *Biochemistry* 22, 3581-3586.
- Wilkinson, A. J., Fersht, A. R., Blow, D. M., Carter, P., & Winter, G. (1984) *Nature* 307, 187-188.

## Accelerated Publications

### Role of Tyrosine M210 in the Initial Charge Separation of Reaction Centers of *Rhodobacter sphaeroides*<sup>†</sup>

Ulrich Finkele, Christoph Lauterwasser, and Wolfgang Zinth  
*Physik Department der Technischen Universität, D-8000 München 2, FRG*

Kevin A. Gray and Dieter Oesterhelt\*

*Max-Planck-Institut für Biochemie, D-8033 Martinsried, FRG*

Received May 22, 1990; Revised Manuscript Received July 12, 1990

**ABSTRACT:** Femtosecond spectroscopy was used in combination with site-directed mutagenesis to study the influence of tyrosine M210 (YM210) on the primary electron transfer in the reaction center of *Rhodobacter sphaeroides*. The exchange of YM210 to phenylalanine led the time constant of primary electron transfer to increase from  $3.5 \pm 0.4$  ps to  $16 \pm 6$  ps while the exchange to leucine increased the time constant even more to  $22 \pm 8$  ps. The results suggest that tyrosine M210 is important for the fast rate of the primary electron transfer.

The primary photochemical event during photosynthesis of bacteriochlorophyll (Bchl)-containing organisms is a light-induced charge separation within a transmembrane protein complex called the reaction center (RC). The crystal structures of RC's from *Rhodopseudomonas (Rps.) viridis* and *Rhodobacter (Rb.) sphaeroides* have been solved to high resolution [reviewed in Deisenhofer and Michel (1989), Chang et al. (1986), Tiede et al. (1988), and Rees et al. (1989)]. The RC from *Rb. sphaeroides* contains three protein subunits referred to as L, M, and H, according to their respective mobilities in SDS-polyacrylamide gels. Associated with the L and M subunits are the cofactors, consisting of four Bchl *a*, two bacteriochlorophyllin (Bph) *a*, one atom of non-heme ferrous iron, two quinones ( $Q_A$  and  $Q_B$ ), and in some species one carotenoid [reviewed in Parson (1987) and Fehér et al.

(1989)]. The cofactors are arranged in two branches (Figure 1) with an approximate  $C_2$  axis of symmetry. The kinetic data support a model in which the primary electron transfer proceeds after light absorption by the primary donor [a special pair of Bchl referred to as P; reviewed in Kirmaier and Holten (1987)]. The absorption of light generates the excited electronic state  $P^*$ , which has a lifetime of approximately 3 ps. An electron is transferred from P along only one branch (the so-called A-branch). It is generally accepted that after approximately 3 ps the electron arrives at the Bph on the A-side ( $H_A$ ) and after 220 ps it reaches  $Q_A$ . The role of the accessory Bchl located between P and  $H_A$  (referred to as  $B_{A1}$ ) has not been definitely assigned. Recently, we have shown that at room temperature an additional kinetic ( $\tau = 0.9$  ps) component is detectable (Holzapfel et al., 1989). The spectral properties and the kinetic constants lead to the conclusion that the corresponding intermediate is the radical pair  $P^*B_{A1}^-$  (Holzapfel et al., 1990).

Additional intriguing points concerning the process of

\* Financial support was from the Deutsche Forschungsgemeinschaft. SFB 143.

† To whom correspondence should be addressed.



## SCIENCE'S COMPASS

prediction methods deduce structure directly from sequence. The approaches are quite different and should not be confused. Their levels of success also differ markedly.

### Function prediction through pattern recognition

Tools for similarity searching are standard components of the sequence annotator's armory. Sequence similarity programs may seek pairwise similarities in large sequence repositories or search for conserved patterns in gene family databases (2–5). Gene family databases allow more specific functional diagnoses to be made than is possible by pairwise searching. They are based on the principle that related sequences can be aligned to find regions (motifs) that show little variation. These motifs usually reflect some vital structural or functional role (see the figure), and they can be used to derive diagnostic family signatures. Sequences can then be searched against databases of such signatures to see whether they can be assigned to known families. Gene family databases have recently been integrated to create a unified protein family resource (6), facilitating the inference of function by identifying homologous relationships.

The term "homology," is often used incorrectly. Sequences are homologous if they are related by divergence from a common ancestor (7). Conversely, analogy relates to the acquisition of common structural or functional features via convergent evolution from unrelated ancestors. For example,  $\beta$  barrels occur in soluble serine proteases and integral membrane proteins, despite their different architectures; they share no sequence or functional similarity. Similarly, the enzymes chymotrypsin and cathepsin share groups of catalytic residues with almost identical spatial geometries, but they have no other sequence or structural similarities. Homology is not a measure of similarity, but rather an absolute statement that sequences have a divergent rather than a convergent relationship. This is not just a semantic issue because imprecise use of the term obscures evolutionary relationships. In comparing structures, the same arguments apply. Structures may be similar, but common evolutionary origin remains a hypothesis until supported by other evidence; the hypothesis may be correct or mistaken, but the similarity is a fact (8).

Among homologous sequences, we can distinguish orthologs (proteins that usually perform the same function in different species) and paralogs (proteins that perform different but related functions within one organism). Orthologs allow investigation of cross-species relationships, whereas paralogs, which arise via gene duplication events, shed light on underlying evolutionary mechanisms because the duplicated genes follow separate

evolutionary pathways and new specificities evolve through variations and adaptation. Such complexity presents real challenges for bioinformatics. When analyzing a database search, it may be unclear how much functional annotation can be legitimately inferred by a query sequence, and whether the best match turned up by the search is the true ortholog or a paralog. This difficulty is the source of numerous annotation errors.

Further complications result from the domain and/or modular nature of many proteins. Modules are autonomous folding units that often function as protein building blocks, forming multiple combinations of the same module or modules of different modules. They can confer a variety of functions on the parent protein. If the best hit in a database search is a match to a single domain or module, it is unlikely that the function annotation can be propagated from the parent protein to the query sequence.

In using modules to confer different functionalities, Nature uses old fashioned to create new systems. The complexity of such systems poses important problems for computational approaches because the properties of a system can be explained by but not deduced from those of its components (9, 10). The presence of a module tells little of the function of the complete system; knowledge about components of a module does not allow us easily to predict a missing one, and modules in different proteins do not always perform the same function.

Many other factors also complicate function assignment: gene functions may be redundant, nonorthologous displacement can replace genes with unrelated but functionally analogous genes, horizontal gene transfer can introduce genes from different phylogenetic lineages, and lineage-specific gene loss can eliminate untested genes. Thus, genomes harbor many obstacles to reliable function assignment.

### What is function?

Protein function is context-dependent. Vagueness in using the term has yielded confusing database annotations. It is currently used to refer vaguely to biochemical activities, biological goals, and cellular structure; for example, the function of actin might be described as "ATPase" or "co-component of the cytoskeleton." In an attempt to invoke rigor into the field and better reflect biological reality, independent ontologies such as the Gene Ontology (GO) are under development that aim to define more explicitly the relationships between gene products and biological processes, molecular functions, and cellular components.

Structure prediction and fold recognition  
We have seen that definitions of "genes" differ, making it difficult to count genes

accurately, and that our concepts of "function" differ, making function assignment tricky. It would seem, however, that we can agree on what structures are. They are tangible, measurable things, so should we not be able to predict them reliably?

Structure prediction methods range from computationally intensive strategies that simulate the physical and chemical forces involved in protein folding to knowledge-based approaches that use information from structure databases to build models. Yet the problem of predicting protein structure remains unsolved: knowledge-based techniques typically produce low-resolution models, and no current method yields reliable predictions for remote homologs (11). For small proteins, ab initio methods generate models with substantial segments that resemble the correct fold, but results deteriorate beyond ~100 residues. Today, knowledge-based methods, especially those that combine information from different approaches, give best results (12). The most successful modeling and fold recognition studies have balanced better algorithms with appropriate levels of manual intervention (13).

Prediction methods do not work well because we do not fully understand how the primary structure of a protein determines its tertiary structure. Structural genomics projects will gradually lessen our reliance on prediction, because they aim to provide experimental structures or models for every protein in all completed genomes (although membrane protein structures will be difficult to obtain because they are difficult to crystallize). We must keep in mind, however, that structure alone will not inherently tell us function (see the figure). For example, determining the structure of a hypothetical protein and discovering that it binds ATP (14) may shed light on possible aspects of its functionality, but such information does not reveal its specific biological function.

### What is structure?

In the context of fold recognition and prediction, it is important to be precise about what we mean by "structure." For example, is a prediction a "good" prediction if it correctly reproduces all atomic positions, the topology (connectivity of secondary structures), the architecture (gross arrangement of secondary structures), or merely the structural class (mainly *C*, mainly *B*, etc.)? Where does a "reasonably good" prediction fall in this hierarchy, and what level of structural detail does a "rough near miss" (15) reveal? Using such imprecise words blurs comprehension, making it difficult to evaluate what a good prediction really is.

TECHSIGHTING  
SOFTWAREConquering by  
Dividing

**Outlook**  
In "predicting" genes, protein functions, and structures, it is helpful to define our terms precisely and be honest about our achievements. Otherwise, we will continue to be baffled by paradoxical new prediction methods that yield >80% error rates. Gene identification, structure prediction, and functional inference are nontrivial computational tasks, but with the relentless accumulation of sequence data, improvements continue to be made in all areas.

Nature functions by integration, and the adoption of a more holistic view of complex biological systems is an essential next step for bioinformatics. To get the most from genomic data, we need to take account of information on the regulation of gene expression, metabolic pathways, and signaling cascades. Proteins do not work in isolation but are involved in interrelated networks. Unraveling these networks and their interactions will be vital to our understanding of normal and pathologic cell development, and will help us create an integrated mapping between genotype and phenotype.

Genomic-based drug discovery is heavily dependent on accurate functional annotation. Toward this end, bioinformatics will need to deliver highly integrated, interoperable databases (and data "warehouses") that allow the user to reason over disparate data sources and ultimately enable knowledge-based inference and innovation. The more genome annotation is automated, the greater will be the need for collaboration between software developers, annotators, and experimentalists. And the more data we have to handle, the more rigorous we must be in our thinking (and writing) if we are to make sense of the results. Sequence-structure-function bioinformatics does not yet yield all the answers, but a future holistic approach should help fuse today's glimmings of knowledge into a new dawn of understanding.

## References and Notes

1. M. G. Rosen et al., *Science*, **284**, 423 (2000).
2. E. Weintraub et al., *Science*, **284**, 2112 (1999).
3. T. L. Saenger et al., *Proteins*, **38**, 262 (2000).
4. A. Katsanis et al., *Proteins*, **40**, 283 (2000).
5. J. Hordijk et al., *Proteins*, **40**, 228 (2000).
6. D. C. Casals et al., *Science*, **284**, 424 (2000).
7. W. C. Rutter, *Proc. Natl. Acad. Sci. USA*, **73**, 99 (1976).
8. G. E. Rosell et al., *Cell*, **50**, 667 (1987).
9. F. Jencik, *Schweiz. Med. Wochenschr.*, **96**, 183 (1987).
10. J. S. Gitter et al., *Science*, **284**, 424 (2000).
11. P. A. McLoone et al., *Nature Genet.*, **23**, 13 (2000).
12. B. Rost and S. O'Donnell, *Comput. Appl. Biomed.*, **12**, 203 (2000).
13. B. Rost, *J. Mol. Biol.*, **294**, 193 (2000).
14. M. J. E. Stoeber et al., *Curr. Opin. Prot. Biol.*, **10**, 364 (1999).
15. L. M. Reinhold et al., *Proc. Natl. Acad. Sci. U.S.A.*, **92**, 15185 (1995).
16. E.A. Chitwood et al., *Comput. Chem.*, **24**, 499 (2000).
17. Single-letter abbreviations for the amino acid residues are: A, Alanine; C, Cysteine; D, Aspartic Acid; E, Glutamic Acid; F, Phenylalanine; G, Glycine; H, Histidine; I, Isoleucine; K, Lysine; M, Methionine; N, Asparagine; P, Serine; Q, Threonine; R, Arginine; S, Tyrosine; T, Threonine; V, Valine; W, Tryptophan; and Y, Tyrosine.

version of the program for Macintosh and Solaris systems are planned.

The benefits of the Popular Power scheme for distributed computing tasks do not accrue solely to the user whose computer is used. The flexible nature of Popular Power's design provides access for businesses, scientists, and anyone with massive computing projects to computing power that is potentially far greater than they would gain from a fixed piece of hardware. Personal computer users might be able to select which commercial job to run through Popular Power Worker depending on the return offered by the originating contractor. A key to the success of the computing model is likely to be the price Popular Power demands for acting as the interface between the computing project creators and the personal computer users.

In summary, the current version of Popular Power Worker is still in the testing phase and users may find the software unstable. Tech-savvy personal computer enthusiasts are best suited to test the current pre-release product. The remaining users are advised to wait at least for the official release of the software.

—KEVIN AHERN

Department of Biochemistry and Biophysics, Oregon State University, Corvallis, OR 97331, USA. E-mail: [sherd@oregonstate.edu](mailto:sherd@oregonstate.edu)

## References

1. J. Kaiser, *Science*, **262**, 839 (1998).

TECHSIGHTING  
SOFTWARE

## Eyes on the Skies

The orbital space above Earth contains an astonishing collection of man-made satellites. Tracking all of these objects is no small task. Liftoff is a NASA Web site that provides several software tools to locate, track, and identify Earth-orbiting satellites. At the Web site, three programs are available:

J-Pass (identifies satellites passing overhead); J-Track (allows one to track orbiting objects); and J-Track 3D (allows one to view satellite orbiting Earth from a perspective far away in space). Each of these platform-independent applications is written in Java and is accessible from both Internet Explorer and Netscape.

J-Track, J-Pass 3D,  
and J-Pass  
NASA

<http://thor.gsfc.nasa.gov/jtrack/JTrack.html>

# From genes to protein structure and function: novel applications of computational approaches in the genomic era

Jeffrey Skolnick and Jacquelyn S. Fetrow

The genome-sequencing projects are providing a detailed 'parts list' of life. A key to comprehending this list is understanding the function of each gene and each protein at various levels. Sequence-based methods for function prediction are inadequate because of the multifunctional nature of proteins. However, just knowing the structure of the protein is also insufficient for prediction of multiple functional sites. Structural descriptors for protein functional sites are crucial for unlocking the secrets in both the sequence and structural-genomics projects.

**G**eome-sequencing projects are providing a detailed 'parts list' for life. Unfortunately, this list, a portion of which represents the amino acid sequence of all the proteins in a given genome, does not come with an instruction manual. That is, given the genome's sequences, one does not necessarily know straight away which regions encode proteins, which serve a regulatory role and which are responsible for the structure and replication of the DNA itself.

This is not unlike giving a child a list of parts necessary to create a working automobile. Without the necessary expertise, creating the final, working car from just the listed parts list is a nearly impossible task. Similarly, understanding how to create a complete functioning cell given just the sequence of nucleotides found in an organism's genome is a complex problem.

#### What is a protein function?

After a genome is sequenced and its complete parts list determined, the next goal is to understand the function(s) of each part, including that of the proteins. What do we mean by protein function, the focus of this article?

Function has many meanings. At one level, the protein could be a globular protein, such as an enzyme, hormone or antibody, or it could be a structural or membrane-bound protein. Another level is its biochemical function, such as the chemical reaction and the substrate specificity of an enzyme. The regulatory molecules or cofactors that bind to a protein are also levels of biochemical function.

At the cellular level, the protein's function would involve its interaction with other macromolecules and the function and cellular location of such complexes. There is also the protein's physiological function, that is, in which metabolic pathway the protein is involved or what physiological role it performs in the organism. Finally, the phenotypic function is the role played by the protein in the total organism, which is observed by deleting or mutating the gene encoding the protein.

J. Skolnick [bsk@janelia.fccc.org](mailto:bsk@janelia.fccc.org) is at the Drosophila Plant Science Center, Laboratory of Computational Genetics, 4041 Forest Park Avenue, St Louis, MO 63108, USA. J.S. Fetrow is at ConProMatic, Suite 200, 1830 Columbia Drive, San Diego, CA 92121-3734, USA.

Obviously, the complete characterization of protein function is difficult but efforts are under way at all levels<sup>1–4</sup>, including cellular function<sup>4,5</sup>. In this article, however, we focus on identifying the biochemical function of a protein given its sequence, a problem that is amenable to molecular approaches.

#### Sequence-based approaches to function prediction

The sequence-to-function approach is the most commonly used function-prediction method. This robust field is well developed and, in the interest of space limitations, we will merely present a brief overview.

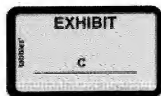
There are two main flavors of this approach: sequence alignment<sup>6,7</sup>, a sequence-matching method, such as Pssm<sup>8</sup>, Blocks<sup>9</sup>, Prints<sup>10,11</sup> and Emotif<sup>12</sup>. Both the alignment and the motif methods are powerful but a recent analysis has demonstrated their significant limitations<sup>13</sup>, suggesting that these methods will increasingly fail as the protein-sequence databases become more diverse.

An extension of these approaches that combines protein-sequence with structural information has been developed and some successes have been reported<sup>14</sup>. However, this method still applies the structural information in a one-dimensional, 'sequence-like' fashion and fails to take into account the powerful three-dimensional information displayed by protein structures.

In addition, proteins can gain and lose function during evolution and may, indeed, have multiple functions in the cell (Box 1). Sequence-to-function methods cannot specifically identify these complexities. Inaccurate use of sequence-to-function methods has led to significant function-annotation errors in the sequence databases<sup>15</sup>.

#### An alternative approach

An alternative, complementary approach to protein-function prediction uses the sequence-to-structure-to-function paradigm. Here, the goal is to determine the structure of the protein of interest and then to identify the functionally important residues in that structure. Using the chemical structure itself to identify functional sites is more in line with how the protein actually works.



In a sense, this is one long-term goal of 'structural genomics' projects<sup>18,19</sup>, which are designed to determine all possible protein folds experimentally, just as genome-sequencing projects are determining all protein sequences<sup>20</sup>. This is in contrast to traditional structural-biology approaches, in which one knows the protein's function first and only then, if the function is sufficiently important, determines its structure.

It is implicitly assumed that having the protein's structure will provide insights into its function, thereby furthering the goals of the human genome-sequencing project. However, knowing the protein's three-dimensional structure is insufficient to determine its function (Box 2). What we really need to analyse and predict the multifunctional aspects of proteins is a method specifically to recognize active sites and binding regions in these protein structures.

#### Active-site identification

In order to use a structure-based approach to function prediction, one must identify the key residues responsible for a given biochemical activity. For many years, it has been suggested that the active sites in proteins are better conserved than the overall fold. Taken to the limit, this suggests that one could not only identify distant ancestors with the same global fold and the same activity but also proteins with similar functions but distantly related, or possibly unrelated, global folds.

The validity of this suggestion was demonstrated empirically by Nussinov and co-workers, who showed that the active sites of eukaryotic serine proteases, subtilisins and sulfhydryl proteases exhibit similar structural motifs<sup>21</sup>. Furthermore, in a recent modeling study of *Saccharomyces cerevisiae* proteins, protein functional sites were found to be more conserved than other parts of the protein models<sup>22</sup>. Similarly, it has been demonstrated that the catalytic triad of the  $\alpha/\beta$  hydrolases is structurally better conserved than other histidine-containing triads<sup>23</sup>. A comparison of the structure of the hydrolase catalytic triad to other histidine-containing triads shows a distinct bimodal distribution, while a similar analysis done with a randomly selected triad shows a unimodal distribution (Fig. 1).

Kasava and Thornton<sup>24</sup> generalised this example by creating structural analogs of a few Prosite sequence motifs<sup>10</sup>. For the 20 most-frequently occurring Prosite patterns, the associated local structure is quite distinct. These results provide clear evidence that enzyme active sites are indeed more highly conserved than other parts of the protein.

#### Identifying active sites in experimental structures

Historically, several groups have attempted to identify functional sites in proteins; their efforts were directed at protein engineering or building functional sites in places where they did not previously exist. This has been successfully accomplished for several metal-binding sites<sup>25–33</sup>. However, highly accurate functional-site descriptors of the backbone and side-chain stances were required, fueling the belief that significant steric detail is needed in site descriptors for function identification.

Highly detailed residue side-chain descriptors of the active sites of serine proteases and related proteins have been used to identify functional sites<sup>34</sup>. The use of these highly detailed motifs has led to the identification of

#### Box 1. Proteins are multifunctional

A common protein characteristic that makes functional analysis based only on homology especially difficult is the tendency of proteins to be multifunctional. For instance, lactate dehydrogenase binds NAD, substrate and zinc, and performs a redox reaction. Each of these occurs at different functional sites that are in close proximity and the combination of all four sites creates the fully functional protein.

Other examples of multifunctional proteins are nucleic-acid-binding proteins. For instance, DNA regulatory proteins often contain a DNA-binding domain, a dimerization domain and a domain that bind regulatory proteins such as sigma factors or RNA<sup>35</sup>. The BC ribosomal proteins exhibits a proteolytic function as well as an RNA-binding function<sup>36,37</sup>. Transcription factors are also complex, multifunctional proteins<sup>38,39</sup>. It is becoming increasingly important to recognize each of these different functions of gene products of a newly sequenced gene.

The serine-threonine-phosphatase superfamily is a prime example of the difficulties of using standard sequence analysis to recognize the multiple functions found in single proteins. This large protein family is divided into a number of subfamilies, all of which contain an essential phosphatase active site. Subfamilies I, II and III contain 420 or more sequence identities between them<sup>40</sup>. However, the identity of these subfamilies is apparently regulated differently in the case<sup>41–47</sup> and observation suggests that there are different functional sites at which regulation can occur. Because the sequence identity between subfamilies is so high, standard sequence-similarity methods could easily misclassify new sequences as members of the wrong subfamily if the functional sites are not carefully considered, as was recently demonstrated<sup>42</sup>.

These are but a few examples of the multifunctionality of proteins. The recognition of this multifunctional nature is of critical importance to the genetics field. Useful functional-annotation methods must consider all of the specific functions in a given protein and will not just provide a general classification of function.

several novel functional sites in known, high-quality protein structures<sup>34,35</sup>. More automated methods for finding spatial motifs in protein structures have also been described<sup>21,34–36</sup>.

Unfortunately, most of these methods require the exact placement of atoms within protein backbones and side chains, and so have not been shown to be relevant to inexact predicted structures. Recently, however, we described the production of fuzzy, inexact descriptors of protein functional sites<sup>33</sup>. As we wish to apply the descriptors to experimental structures as well as to predicted protein models, we used only carbon atoms and 'side-chain' centers-of-mass positions. We call these descriptors 'fuzzy functional forms' (FFF) and have created them for both the disulfide-oxidoreductase<sup>33,41</sup> and  $\alpha/\beta$ -hydrolase catalytic active sites<sup>33</sup>.

The disulfide-oxidoreductase FFF was applied to screen high-resolution structures from the Brookhaven protein database<sup>42</sup>. In a dataset of 364 protein structures, the FFF accurately identified all proteins known to exhibit the disulfide-oxidoreductase active site<sup>43</sup>. In a second dataset of 1501 proteins, the FFF again accurately identified all proteins with the active site. In addition, it identified another protein, 1fmu, a serine-threonine phosphatase. This result was initially discouraging but subsequent sequence alignment and clustering analysis strongly suggested that this putative site might indeed be a site of redox regulation in the serine-threonine phosphatase-1 subfamily<sup>43</sup>. If confirmed by experiment, this result will highlight the advantages of using structural descriptors to analyze multiple functional sites in proteins. It will also highlight the fact that human

**Box 2. Knowing a protein's structure does not necessarily tell you its function**

Because proteins can have similar folds but different functions<sup>6,9</sup>, determining the structure of a protein may or may not tell you something about its function. The most well-studied example is the ( $\alpha/\beta$ ) barrels, which of these, of which triose-phosphate isomerase (TIM) is the archetypal representative. Members of this family have similar overall structures but different functions, including different active sites, substrate specificities and cofactor requirements<sup>2,7</sup>.

Is this example common? Our own analysis of the 1997 SCOP database<sup>14</sup> shows that the five largest fold families are the ferredoxin-like, the ( $\alpha/\beta$ ) barrels, the knottins, the immunoglobulin-like and the flavodoxin-like fold families with 22, 18, 10 and 9 superfamilies, respectively (Fig. 1). In fact, 57 of the 94 SCOP fold families consist of multiple superfamilies. These data do not show the tip of the iceberg, because each superfamily is further composed of protein families and each individual family can have radically different functions. For example, the ferredoxin-like superfamily contains families identified as Fe-S ferredoxins, ribosomal proteins, DNA-binding proteins and phosphatases, among others.

After this article was submitted, a much more detailed analysis of the SCOP database was published<sup>15</sup>. This finds a much larger set of structure-correlated functional classes, but also finds a number of ubiquitous functional protein structures that occur across a number of families. The article provides a useful analysis of the confidence with which structure and function can be correlated<sup>15</sup>. Knowing the protein structure by itself is insufficient to annotate a number of functional classes and is also insufficient for annotating the specific details of protein function.

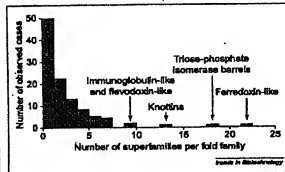


Figure 1

Histogram of the numbers of superfamilies found in each SCOP fold family. These data clearly show that proteins with similar structures can have different functions and demonstrates the difficulty of assigning protein function based simply on the three-dimensional structure. The data were taken from the 1997 distribution of SCOP (<http://scop.mrc-lmb.cam.ac.uk/scop>). For a more detailed analysis, see Ref. 72.

observation alone is no longer adequate for identifying all functional sites in known protein structures.

To date, the use of structure to identify function has largely focused on high-resolution structures and highly detailed descriptors of protein functional sites. However, the creation of inexact descriptors for functional sites opens the way to the application of these methods to inexact, predicted protein models. The question remains: how good does a model have to be in order to use PFPs to identify its active sites?

**The state of the art in structure-prediction methods**

For proteins whose sequence identity is above ~30%, one can use homology modeling to build the structure<sup>16</sup>. However, structure prediction is far more difficult for proteins that are not homologous to proteins with known structure. At present, there are two approaches for these sequences: *ab initio* folding<sup>17,18</sup> and threading<sup>19,20</sup>.

In *ab initio* folding, one starts from a random conformation and then attempts to assemble the native structure. As this method does not rely on a library of pre-existing folds, it can be used to predict novel folds. The recent CASP3 protein-structure-prediction experiment (<http://PredictionCenter.Berkeley.gov/CASP3>) involved the blind prediction of the three-dimensional structure of proteins whose actual structure was about to be experimentally determined. These results indicate that considerable progress has been made<sup>21,22</sup>. For helical and  $\alpha/\beta$  proteins with less than 110 residues, structures were often predicted whose backbone root-mean-square deviation (RMSD) from native ranged from 4–7 Å. Progress is being made with  $\beta$  proteins, too, although they remain problematic. Because *ab initio* methods can identify novel folds, these methods could be used to help to select sequences likely to yield novel folds in experimental structural-genomics projects.

Another approach to tertiary-structure prediction is threading. Here, for the sequence of interest, one attempts to find the closest matching structure in a library of known folds<sup>23,24</sup>. Threading is applicable to proteins of up to 500 residues or so and is much faster than *ab initio* approaches. However, threading cannot be used to obtain novel folds.

**Ab initio predicted models can be used for automatic protein-function prediction**

The results of the recent CASP3 competition suggest that current modeling methods can often (but not always) create inexact protein models. Are these structures useful for identifying functional sites in proteins? Using the *ab initio* structure-prediction program MONSSTER, the tertiary structure of a glutaredoxin, Igo, was predicted<sup>25</sup>. For the lowest-energy model, the overall backbone RMSD from the crystal structure was 5.7 Å.

To determine whether this inexact model could be used for function identification, the sets of correctly and incorrectly folded structures were screened with the FPP for disulfide-oxidoreductase activity<sup>26</sup>. The FPP uniquely identified the active site in the correctly folded structure but not in the incorrectly folded ones (Fig. 2). This is a proof-of-principle demonstration that inexact models produced by *ab initio* prediction of structure from sequence can be used for the subsequent prediction of biochemical function. Of course, improvements in the method have to be made before such predictions can be done on a routine basis.

**Use of predicted structures from threading in protein-function prediction**

At present, practical solutions preclude folding an entire genome of proteins using *ab initio* methods<sup>27</sup>. Threading is more appropriate for achieving the requisite high-throughput structure prediction. Thus, a standard threading algorithm<sup>28</sup> has been used to screen all

proteins in nine genomes for the disulfide-oxidoreductase active site described above.

First, sequences that aligned with the structures of known disulfide oxidoreductases were identified. Then, the structure was searched for matches to the active-site residues and geometry. For those sequences for which other homologs were available, a sequence-conservation profile was constructed<sup>22</sup>. If the putative active-site residues were not conserved in the sequence subfamily to which the protein belongs, that sequence was eliminated. Otherwise, the sequence is predicted to have the function.

Using this sequence-to-structure-to-function method, 99% of the proteins in the nine genomes that have known disulfide-oxidoreductase activity have been found. From 10% to 30% more functional predictions are made than by alternative sequence-based approaches; similar results are seen for the  $\alpha/\beta$  hydrolases<sup>23</sup>. Surprisingly, in spite of the fact that threading algorithms have problems generating good sequence-to-structure alignments, active sites are often accurately aligned, even for very distant matches. This observation would agree with the above experimental results indicating that active sites are well conserved in protein structures.

Importantly, the false-positive rate when using structural information is much lower than that found using sequence-based approaches, as demonstrated by a detailed comparison of the FFP structural approach and the Blocks<sup>24</sup> sequence-matching approach (N. Siew et al., unpublished). In this study, three sequences in eight genomes (including *Bacillus subtilis*) were analyzed for disulfide-oxidoreductase function using the disulfide-oxidoreductase FFP, the thioesterase block 00194 and the glutaredoxin Block 00195. If we assume that those sequences identified by both the FFP and Blocks are 'true positives', we find 13 such sequences in the *B. subtilis* genome.

There is no experimental evidence validating all of these 'true positives' and so they are more accurately termed 'consensus positives'. In order to find these 13 'consensus positive' sequences, the FFP hits serve false positives. On the other hand, Blocks hits 23 false positives (Fig. 3). It was previously suggested that the use of a functional requirement adds information to threading and reduces the number of false positives<sup>23</sup>. These data, including the data shown in Fig. 3, validate this claim on a genome-wide basis.

Of course, no genome has had the function of all of its proteins experimentally confirmed, it is impossible to know how many other proteins with the specified biochemical function were not properly identified. This is a critical question for researchers attempting to predict protein function. Experimental confirmation will be needed to validate this or any other method fully. This points out the need for closely coupling computational function-prediction algorithms with experiments.

#### Weaknesses of using the sequence-to-structure-to-function method of function prediction

Based on studies to date, the identification of enzymatic activity requires a model in which the backbone RMSD from native near the active sites is about 4–5 Å. Predicted models are better at describing the geometry in the core of the molecule than in the loops and so

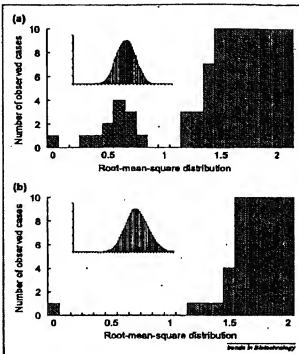


Figure 1

The distribution of root-mean-square distributions (RMSD) between the hydrolase catalytic triad and all other histidine-containing triads shows a bimodal distribution [a]; by contrast, the RMSD between a randomly selected (non-catalytic) triad and all other histidine-containing triads has a unimodal distribution [b]. The His-Ser-Asp catalytic triad in the protein 1\_gpl (PDB space) [a] and a random histidine-containing triad from 40gpa (glutamine-asparaginase) [b] were structurally aligned to all His-containing triads in a database of 1037 proteins<sup>25</sup>. Actual  $\alpha/\beta$ -hydrolase active sites [a] and the 40gpa site [b] are indicated by blue bars; other histidine triads that are not active sites are indicated by red bars. None of the sites found by matching to the 40gpa were hydrolase active sites. Inset graphs show the full distribution.

predicting the function of a protein whose active site is in loops may be a problem. Also, the method can currently only be applied to enzyme active sites; substrate and ligand-binding sites have not yet been identified using the inexact models. Techniques that will further refine inexact protein models will be quite useful in taking the protein analysis to the next step.

#### Conclusions

Although sequence-based approaches to protein-function prediction have proved to be very useful, alternatives are needed to assign the biochemical function of the 30–50% of proteins whose function cannot be assigned by any current methods. One emerging approach involves the sequence-to-structure-to-function paradigm. Such structures might be provided by structural-genomics projects or by structure-prediction algorithms. Functional assignment is made by screening the resulting structure against a library of structural descriptors for known active sites or binding regions.

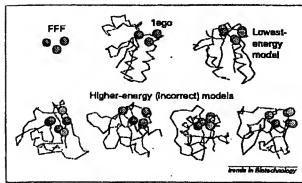


Figure 2

Application of the disulfide-oxidoreductase fuzzy functional form (FFF) to ab initio models of glutaredoxin created by the program MONSTER shows that the FFF can distinguish between correctly folded and misfolded (higher-energy) models. The FFF is shown as two orange balls (representing the cysteines) and a blue ball (representing the proline). The protein models are shown as magenta wire models with the active-site cysteines and proline shown as yellow and cyan balls, respectively. The FFF clearly distinguishes the correct active site in the crystal structure of the glutaredoxin lego and the correctly folded, lowest-energy model. The FFF does not match to the active sites of any of the higher energy, misfolded structures, four of which are shown here.

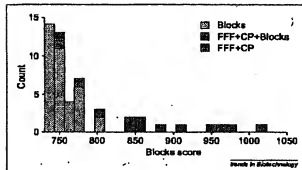


Figure 3

Analysis of the *Bacillus subtilis* genome using the thiodredoxin block D0194. The Blocks score (computed using the publicly available BLMP3 program) is plotted on the x axis and the number of sequences found in each scoring bin is plotted on the y axis. Those sequences identified as 'consensus positives' (identified by both the fuzzy functional form (FFF) and the Block) are shown as red bars. One additional sequence found by the FFF, which is likely to be a true positive, is shown as a blue bar. All other sequences, putative 'false positives', are shown as yellow bars. Using the Blocks score at which all 13 of the 'consensus positives' are found, 23 false positives are also found. In its analysis of the *B. subtilis* genome, the FFF identifies only seven false positives along with the same 13 'consensus positives' (data not shown).

Detailed descriptors will only work on the experimentally determined, high-quality structures. Ideally, however, the descriptors should work on both experimental structures and the coarser models provided by tertiary-structure-prediction algorithms.

The advantages of such an approach are that one need not establish an evolutionary relationship in order to assign function, that more than one function can be

assigned to a given protein [an issue of major importance, because proteins are multifunctional (Box 1)] and, ultimately, that having a structure can provide deeper insight into the biological mechanism of protein function and regulation. The disadvantages are that one needs to have the protein's structure before a function can be assigned and that the approach is limited to those functions associated with proteins with at least one solved structure, so that a functional-site descriptor can be constructed.

In this sense, structure-to-function assignment can be thought of as 'functional threading' – find the active-site match in a library of descriptors for known protein active sites. This is the first step in the long process of using structure to assign all levels of function, a goal that is made increasingly important with the emergence of structural genomics. Based on the progress to date, it is apparent that structure will play an important role in the post-genomic era of biology.

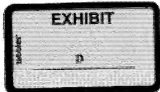
#### Acknowledgment

We thank L. Zhang for producing the data in Box 2 and Fig. 1.

#### References

- Gurd, F.R.N. and Rodriguez, T.M. (1979) Models in proteins. *Adv. Protein Chem.* 33, 73–115.
- Laskowski, R.A. *et al.* (1996) X-SITE: use of empirically derived steric packing preferences to identify favourable interaction regions in the binding sites of proteins. *J. Mol. Biol.* 259, 175–201.
- Wallace, A.C. *et al.* (1996) Derivation of 3D coordinate templates for protein structure descriptor generation. *Proteins* 24, 1071–1013.
- Hershko, S. and Henikoff, J.G. (1973) Assessment sensitivity to peptide blocks for database searching. *Nucleic Acids Res.* 1, 6563–6572.
- Riley, M. (1992) Functions of gene products of *Escherichia coli*. *Mol. Microbiol.* 57, 862–873.
- Karp, P.D. and Riley, M. (1993) Representations of metabolic knowledge. *Anal. Biochem.* 217, 207–215.
- Altschul, S.F. *et al.* (1990) Basic local alignment search tool. *J. Mol. Biol.* 215, 403–410.
- Pearson, W.R. (1990) Effective protein sequence comparison. *Methods Enzymol.* 264, 227–258.
- Sommer, B.S. and Collins, J.P. (1993) *Biowarping Research Unit*, University of Edinburgh, Edinburgh, UK.
- Barlow, A. *et al.* (1995) The PROSITE database, in status in 1995. *Nucleic Acids Res.* 24, 189–196.
- Henikoff, S. and Henikoff, J.G. (1994) Protein family classification based on searching a database of blocks. *Genetics* 139, 97–107.
- Henikoff, S. and Henikoff, J.G. (1994) PROSITE: A resource of protein motif fingerprints. *Nucleic Acids Res.* 22, 385–396.
- Armwood, T.K. *et al.* (1997) Novel developments with the PRINTS protein fingerprint database. *Nucleic Acids Res.* 25, 213–216.
- Nebl-Manning, C.C. *et al.* (1998) Highly specific protein sequence motif for genome analysis. *Proc. Natl. Acad. Sci. U.S.A.* 95, 5863–5871.
- Fenton, J.S. and Skolnick, J. (1990) Method for prediction of protein function from sequence using the sequence-to-structure-to-function paradigm with application to glutaredoxin/thioredoxin superfamily proteins. *J. Mol. Biol.* 211, 949–961.
- Ye, L. *et al.* (1998) A combined identification method that combines protein sequence and sequence information. *Proteins* 31, 2499–2510.
- Bork, P. and Eisenberg, A. (1995) Go hunting in sequence databases but watch out for traps. *Trends Genet.* 11, 425–427.
- Gasteiger, T. (1998) Structural genomics: bioinformatics in the driver's seat. *Nat. Biotechnol.* 16, 625–627.
- McKusick, V.A. (1997) Genomics: structural and functional studies of genomes. *Genome* 45, 244–249.
- Monteiro, G.T. and Anderson, S. (1999) Structural genomics: keynotes for a human proteome project. *Nat. Rev. Genet.* 6, 11–12.

- 21 Fischer, D. et al. (1994) Three-dimensional sequence-independent structural comparison of a serine protease against the crystallographic database reveals active site similarities: potential implications to evolution and to protein folding. *Proteins* **14**, 3, 769–778.
- 22 Sanchez, R. and Sali, A. (1998) Large-scale protein structure modeling of the *Escherichia coli* proteome. *Proc. Natl. Acad. Sci. U.S.A.* **95**, 13597–13602.
- 23 Zhou, L. et al. (1998) Predictive analysis of *E. coli* proteins for membrane protein families. *Proc. Natl. Acad. Sci. U.S.A.* **95**, 535–548.
- 24 Karayannidis, A. and Thornton, J.M. (1998) Three-dimensional structure analysis of Prosite patterns. *J. Mol. Biol.* **284**, 1672–1691.
- 25 Caldera, C.D. et al. (1997) The rational design and construction of a cuboidal iron-malate protein. *Proc. Natl. Acad. Sci. U.S.A.* **94**, 6435–6440.
- 26 Plaza, A.L. et al. (1997) Construction of a catalytically active iron-superoxide dismutase by rational protein design. *Proc. Natl. Acad. Sci. U.S.A.* **94**, 5363–5367.
- 27 Hellmuth, M.W. and Richards, F.M. (1991) Construction of new ligand binding sites in proteins of known structure: (I) computer-aided modeling of sites with pre-defined functions. *J. Mol. Biol.* **222**, 763–785.
- 28 Hollings, H.W. et al. (1991) Construction of new ligand binding sites in proteins of known structure: (II) grafting of a buried trinucleotide metal binding site into *Escherichia coli* thioredoxin. *J. Mol. Biol.* **222**, 787–803.
- 29 Klemke, L. and Regan, L. (1995) Characterisation of mixed binding by a designed metallochaperone: single ligand substitutions at a tetrahedral Cys<sup>100</sup> residue. *Protein Eng.* **8**, 1099–1100.
- 30 Klemke, L. et al. (1995) Mixed metal binding proteins by design. *Nature Struct. Biol.* **2**, 364–373.
- 31 Putton, E. and Regan, L. (1998) The de novo design of a rubredoxin-like Fe protein. *Proteins* **7**, 1939–1946.
- 32 Cowdell, M.W. et al. (1995) Spectroscopic studies on the designed metal-binding sites of the GCN4 single chain bZIPs. *J. Am. Chem. Soc.* **117**, 5627–5634.
- 33 Holden, S. and Croft, C.S. (1996) Regulation of proteolytic activity by multiple redox metal binding loops. *J. Am. Chem. Soc.* **118**, 1227–1228.
- 34 Walker, A.C. et al. (1997) TESS: a graphical heuristic algorithm for deriving 3D coordinate complexes for searching structural database application to enzyme active sites. *Proteins* **6**, 2309–2323.
- 35 Kleywegt, G.J. (1999) Recognition of spatial motifs in protein structures. *J. Mol. Biol.* **285**, 1867–1877.
- 36 Mason, Y. and Nishikawa, K. (1994) Protein structural similarities predicted by a sequence-structure compatibility method. *Proteins* **23**, 2025–2033.
- 37 Rand, R.B. (1999) Detection of protein three-dimensional similarities: a new example of convergent evolution. *J. Mol. Biol.* **294**, 1251–1257.
- 38 Ho, K.F. et al. (1997) Three-dimensional surfaces fold enzymes associated with aromatic amino acid sequence patterns. *Proteins* **27**, 1387–1390.
- 39 Aravind, P. et al. (1994) A graph-theoretic approach to the identification of functional domains in proteins: detection of common side-chain motifs in protein databases. *J. Mol. Biol.* **236**, 327–344.
- 40 Kalin, S. and Zhai, Z.Y. (1996) Characteristics of diverse residue classes in protein three-dimensional structures. *Proc. Natl. Acad. Sci. U.S.A.* **93**, 8344–8349.
- 41 Putton, J.S. et al. (1999) Functional analysis of the *Escherichia coli* genome using the sequence-to-structure-to-function paradigm: identification of proteins exhibiting the glutathione/thioredoxin disulfide oxidoreductase activity. *J. Mol. Biol.* **292**, 703–711.
- 42 Abrah, E.R. et al. (1997) Structure and Function in Crystallographic Database. In: *Advances in Bioinformatics, Biophysics and Applications* (Allen, P.H. et al., eds.), Disc. Commission of the International Union of Crystallography, Dordrecht/Chichester/Churier.
- 43 Putton, J.S. et al. (1999) Serocore-based functional motif identifies a powerful disulfide oxidoreductase active site in the active/thioredoxin protein phosphatase-1 subfamily. *PASED* **13**, 1866–1874.
- 44 Sali, A. et al. (1993) Evaluation of comparative protein modeling by MODELLER. *Proteins* **23**, 318–326.
- 45 Dyson, C. and Lake, D. (1998) Prediction of local structure in proteins using a library of sequence-structure motifs. *J. Mol. Biol.* **281**, 565–577.
- 46 Shand, D. (1999) The size of the set. *Curr. Biol.* **9**, R205–R209.
- 47 Lee, J. et al. (1999) Calculation of protein conformation by global optimization of a pseudopotency function. *Proteins* **34**(Suppl.), 304–308.
- 48 Orts, A. et al. (1999) *In silico* folding of proteins using sequence-structure motifs. *Proteins* **34**(Suppl.), 309–313.
- 49 Bowie, J.U. et al. (1991) A method to identify protein sequences that fold into a known three-dimensional structure. *Science* **253**, 164–170.
- 50 Finkbergen, A.V. and Reva, B.A. (1991) A search for the most stable folds of protein chains. *Nature* **351**, 497–499.
- 51 Bryant, S.H. and Lawrence, C.E. (1993) An empirical energy function for threading protein sequence through folding motifs. *Proteins* **16**, 92–112.
- 52 Lubotzky, R. and Smith, T.F. (1998) Global optimum protein threading with gapped alignment and empirical pair scoring function. *J. Mol. Biol.* **281**, 641–663.
- 53 Strelak, D.T. et al. (1992) A new approach in protein fold recognition. *Nature* **358**, 86–89.
- 54 Saarinen, M. et al. (1999) Progress in protein structure prediction: assessment of CASP3. *Curr. Opin. Struct. Biol.* **9**, 368–373.
- 55 Miller, R.T. et al. (1996) Protein fold recognition by sequence threading tools and assessment techniques. *PASED* **10**, 171–178.
- 56 Orts, A.R. et al. (1998) Fold assembly of small proteins using Monte Carlo simulation driven by restraints derived from multiple sequence alignment. *J. Mol. Biol.* **277**, 413–418.
- 57 Skolnick, J. et al. (1999) Protein fold recognition and their applications to the protein folding problem. *J. Biomol. Struct. Dyn.* **17**, 201–206.
- 58 Jozwiakowski, L. et al. (1998) Fold prediction by a hierarchy of sequence, threading and modeling methods. *Proteins* **31**, 1431–1440.
- 59 Takahashi, M. et al. (1996) Location of functional domains in the RecA protein overlap of densities and regulation of activities. *Proc. J. Biochem.* **242**, 20–28.
- 60 Leong, L.E. et al. (1993) Human thioredoxin-14 precursor 3C (3Cypc) binds specifically to the 3' non-coding region of the viral RNA: evidence that 3C-type proteases cleave the RNA binding and proteolytically activated. *J. Biol. Chem.* **268**, 25733–25739.
- 61 Marthaler, D.A. et al. (1994) Structure of human rhinovirus 3C protease reveals a tryptic-like polypeptide fold, RNA-binding site and means for cleaving precursor polyproteins. *Cell* **77**, 761–771.
- 62 Ladurner, M. (1997) Multi-functional proteins trigger crosstalk between transcriptional and post-transcriptional processes. *BioEssays* **19**, 903–909.
- 63 Goldberg, J. et al. (1995) Three-dimensional structure of the catalytic unit of protein serine/threonine phosphatase-1. *Nature* **374**, 747–753.
- 64 Montel, M.C. and Walter, G. (1993) Proteins serine/threonine/phosphotyrosine structure, regulation and function in cell growth. *Physiol. Rev.* **73**, 673–699.
- 65 Jia, Z. (1997) Protein phosphorylation: structure and implications. *BioEssays* **19**, 17–26.
- 66 Holman, C.B. and Isbrand, M.P. (1993) Inhibition of protein phosphatase-1 and -2A: two of the major serine/threonine/protein phosphatases involved in cellular regulation. *Curr. Opin. Struct. Biol.* **3**, 934–941.
- 67 Neiman, R. and Lee, E.Y.C. (1993) Reactivity of allylhydroxyl groups of the catalytic subunit of rabbit skeletal muscle protein phosphatase 1 and 2A. *Arch. Biochem. Biophys.* **300**, 24–29.
- 68 Marin, A.C. et al. (1995) Script: a structural classification of protein domains for the investigation of sequences and structures. *J. Mol. Biol.* **247**, 536–540.
- 69 Orengo, C.A. et al. (1997) CATH: a hierachical classification of protein structures. *Structures* **5**, 1043–1100.
- 70 Lask, A.M. et al. (1989) Secondary potentials of  $\alpha/\beta$  proteins: the packing of the interior of the sheet. *Proteins Struct. Funct. Genet.* **5**, 139–148.
- 71 Fisher, G.K. and Peacock, G.A. (1990) The evolution of  $\alpha/\beta$  barrel enzymes. *Trends Biochem. Sci.* **15**, 228–234.
- 72 Hegyi, H. and Gerstein, M. (1999) The relationship between protein structure and function: a comprehensive survey with application to the yeast genome. *J. Mol. Biol.* **288**, 147–164.

**BLAST****Basic Local Alignment Search Tool**

[Edit and Resubmit](#) [Save Search Strategies](#) [Formatting options](#) [Download](#)

Blast 2 sequences

**Protein Sequence (806 letters)**

Results for:  lcl|43901 None(806aa)

Your BLAST job specified more than one input sequence. This box lets you choose which input sequence to show BLAST results for.

**Query ID**

lcl|43901  
 lcl|43901

**Description**

None

**Molecule type**

amino acid

**Query Length**

806

**Subject ID**

43903

**Description**

None

**Molecule type**

amino acid

**Subject Length**

1106

**Program**

BLASTP 2.2.22+ [Citation](#)

**Reference**

Stephen F. Altschul, Thomas L. Madden, Alejandro A. Schäffer, Jinghui Zhang, Zheng Zhang, Webb Miller, and David J. Lipman (1997), "Gapped BLAST and PSI-BLAST: a new generation of protein database search programs", Nucleic Acids Res. 25:3389-3402.

**Reference - compositional score matrix adjustment**

Stephen F. Altschul, John C. Wootton, E. Michael Gertz, Richa Agarwala, Aleksandr Morgulis, Alejandro A. Schäffer, and Yi-Kuo Yu (2005) "Protein database searches using compositionally adjusted substitution matrices", FEBS J. 272:5101-5109.

Other reports: [Search Summary](#) [\[Taxonomy reports\]](#) [\[Multiple alignment\]](#) new

[Search Parameters](#)

Search parameter name	Search parameter value
-----------------------	------------------------

Program	blastp
Word size	3
Expect value	10
Hitlist size	100
Gapcosts	11,1
Matrix	BLOSUM62
Filter string	F

Genetic Code	1
Window Size	40
Threshold	11
Composition-based stats	2

Karin-Altschul statistics

**Params Ungapped Gapped**

Lambda	0.318991	0.267
K	0.133935	0.041
H	0.404134	0.14

## Results Statistics

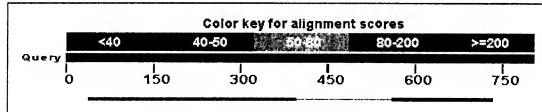
**Results Statistics parameter name Results Statistics parameter value**

Effective search space	809244
------------------------	--------

Graphic Summary**Distribution of 5 Blast Hits on the Query Sequence**

[?]

An overview of the database sequences aligned to the query sequence is shown. The score of each alignment is indicated by one of five different colors, which divides the range of scores into five groups. Multiple alignments on the same database sequence are connected by a striped line. Mousing over a hit sequence causes the definition and score to be shown in the window at the top, clicking on a hit sequence takes the user to the associated alignments. New: This graphic is an overview of database sequences aligned to the query sequence. Alignments are color-coded by score, within one of five score ranges. Multiple alignments on the same database sequence are connected by a dashed line. Mousing over an alignment shows the alignment definition and score in the box at the top. Clicking an alignment displays the alignment detail.



## Dot Matrix View

## Plot of Icl|43901 vs 43903 [?]

This dot matrix view shows regions of similarity based upon the BLAST results. The query sequence is represented on the X-axis and the numbers represent the bases/residues of the query. The subject is represented on the Y-axis and again the numbers represent the bases/residues of the subject. Alignments are shown in the plot as lines. Plus strand and protein matches are slanted from the bottom left to the upper right corner, minus strand matches are slanted from the upper left to the lower right. The number of lines shown in the plot is the same as the number of alignments found by BLAST.



## Descriptions

```

Sequences producing significant alignments:
          Score   E
          (Bits)  Value
lcl|43903  unnamed protein product      62.8  1e-13

```

Alignments Select All Get selected sequences Distance tree of results Multiple alignment [New](#)

>lcl|43903 unnamed protein product  
Length=1106

Score = 62.8 bits (151), Expect = 1e-13, Method: Compositional matrix adjust.  
Identities = 84/382 (21%), Positives = 153/382 (40%), Gaps = 49/382 (12%)

Score = 40.8 bits (94), Expect = 4e-07, Method: Compositional matrix adjust  
Identities = 45/189 (23%), Positives = 75/189 (39%), Gaps = 33/189 (17%)

Sbjct 332 T++V A P P + WFKDN TL + S + RN LT+ RV+ 389  
RSRTLQVVEFEAY--PPPTVLWFKDNRTLGDSSAGEIALSTRNVSETRYVSELTVRVKVA  
Query 729 DGGLYTCQAA 737  
+ G YT +A  
Sbjct 390 EAGHYTMRA 398

Score = 20.4 bits (41), Expect = 0.52, Method: Compositional matrix adjust.  
Identities = 14/67 (20%), Positives = 28/67 (41%), Gaps = 5/67 (7%)

Query 624 IVAFQNDSLQDQGDDYVCSAQDKK---TKKRHCLVKQLIILERMAPMITGNLENQTTTIGE 680  
++ N + D G+Y C+ D + T +R L + + + + E + E  
Sbjct 84 VLTLTNLTGLDTGEYFCFHNSRGLLETDERKRLY--IFVPDPVTVGFLPNDAEELFIFLTE 141  
Query 681 TIEVTCP 687  
E+T P  
Sbjct 142 ITEITIP 148

Score = 20.4 bits (41), Expect = 0.59, Method: Compositional matrix adjust.  
Identities = 7/15 (46%), Positives = 8/15 (53%), Gaps = 0/15 (0%)

Query 684 VTCPASGNTPHITW 698  
V C G P P+I W  
Sbjct 434 VRCRGRGMPPQPNIIW 448

Score = 17.3 bits (33), Expect = 4.7, Method: Compositional matrix adjust.  
Identities = 8/32 (25%), Positives = 14/32 (43%), Gaps = 0/32 (0%)

Query 162 SLCARYPEKRFVPDGNRISWSEIGFTLPSYM 193  
+ + + +KR P S +G LPS++  
Sbjct 699 TFLQHHSDKRRPPSAELYSNALPVGLPLPSHV 730

Select All [Get selected sequences](#) [Distance tree of results](#) [Multiple alignment](#) [NEW](#)

**BLAST****Basic Local Alignment Search Tool**

[Edit and Resubmit](#) [Save](#) [Search Strategies](#) [Formatting options](#) [Download](#)

Blast 2 sequences

**Protein Sequence (806 letters)**

Results for:  Icl|60337 None(806aa)

Your BLAST job specified more than one input sequence. This box lets you choose which input sequence to show BLAST results for.

**Query ID**

Icl|60337  
Icl|60337

**Description**

None

**Molecule type**

amino acid

**Query Length**

806

**Subject ID**

60339

**Description**

None

**Molecule type**

amino acid

**Subject Length**

1091

**Program**

BLASTP 2.2.22+ [Citation](#)

**Reference**

Stephen F. Altschul, Thomas L. Madden, Alejandro A. Schäffer, Jinghui Zhang, Zheng Zhang, Webb Miller, and David J. Lipman (1997), "Gapped BLAST and PSI-BLAST: a new generation of protein database search programs", Nucleic Acids Res. 25:3389-3402.

**Reference - compositional score matrix adjustment**

Stephen F. Altschul, John C. Wootton, E. Michael Gertz, Richa Agarwala, Aleksandr Morgulis, Alejandro A. Schäffer, and Yi-Kuo Yu (2005) "Protein database searches using compositionally adjusted substitution matrices", FEBS J. 272:5101-5109.

Other reports: [Search Summary](#) [\[Taxonomy reports\]](#) [\[Multiple alignment\]](#) NEW

[Search Parameters](#)

Search parameter name	Search parameter value
-----------------------	------------------------

Program	blastp
Word size	3
Expect value	10
Hitslist size	100
Gapcosts	11,1
Matrix	BLOSUM62
Filter string	F

Genetic Code	1
Window Size	40
Threshold	11
Composition-based stats	2

Karlin-Altschul statistics

**Params Ungapped Gapped**

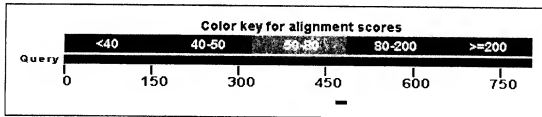
Lambda	0.318991	0.267
K	0.133935	0.041
H	0.404134	0.14

## Results Statistics

Results Statistics	parameter name	Results Statistics	parameter value
Effective search space		799624	

Graphic Summary**Distribution of 1 Blast Hits on the Query Sequence**

An overview of the database sequences aligned to the query sequence is shown. The score of each alignment is indicated by one of five different colors, which divides the range of scores into five groups. Multiple alignments on the same database sequence are connected by a striped line. Mousing over a hit sequence causes the definition and score to be shown in the window at the top, clicking on a hit sequence takes the user to the associated alignments. New: This graphic is an overview of database sequences aligned to the query sequence. Alignments are color-coded by score, within one of five score ranges. Multiple alignments on the same database sequence are connected by a dashed line. Mousing over an alignment shows the alignment definition and score in the box at the top. Clicking an alignment displays the alignment detail.



Dot Matrix View**Plot of lcl|60337 vs 60339 [?]**

This dot matrix view shows regions of similarity based upon the BLAST results. The query sequence is represented on the X-axis and the numbers represent the bases/residues of the query. The subject is represented on the Y-axis and again the numbers represent the bases/residues of the subject. Alignments are shown in the plot as lines. Plus strand and protein matches are slanted from the bottom left to the upper right corner, minus strand matches are slanted from the upper left to the lower right. The number of lines shown in the plot is the same as the number of alignments found by BLAST.

Descriptions

Sequences producing significant alignments:	Score (Bits)	E Value
lcl 60339 unnamed protein product	<u>16.5</u>	7.7

Alignments Select All Get selected sequences Distance tree of results Multiple alignment New

>lcl|60339 unnamed protein product  
Length=1091  
Score = 16.5 bits (31), Expect = 7.7, Method: Compositional matrix adjust.  
Identities = 8/19 (42%), Positives = 8/19 (42%), Gaps = 0/19 (0%)  
Query 472 PGQTSPYACKEWRHVEDFQ 490  
P Q P A E V D Q  
Sbjct 1071 PSQVLP PASPEGETVADLQ 1089

Select All Get selected sequences Distance tree of results Multiple alignment New

**BLAST****Basic Local Alignment Search Tool**[Edit and Resubmit](#) [Save Search Strategies](#) [Formatting options](#) [Download](#)

Blast 2 sequences

**Protein Sequence (806 letters)**Results for:  lcl|40585 None(806aa) 

Your BLAST job specified more than one input sequence. This box lets you choose which input sequence to show BLAST results for.

**Query ID** lcl|40585  
 lcl|40585**Description**

None

**Molecule type**

amino acid

**Query Length**

806

**Subject ID**

40587

**Description**

None

**Molecule type**

amino acid

**Subject Length**

820

**Program**BLASTP 2.2.22+ [Citation](#)**Reference**

Stephen F. Altschul, Thomas L. Madden, Alejandro A. Schäffer, Jinghui Zhang, Zheng Zhang, Webb Miller, and David J. Lipman (1997), "Gapped BLAST and PSI-BLAST: a new generation of protein database search programs", Nucleic Acids Res. 25:3389-3402.

**Reference - compositional score matrix adjustment**

Stephen F. Altschul, John C. Wootton, E. Michael Gertz, Richa Agarwala, Aleksandr Morgulis, Alejandro A. Schäffer, and Yi-Kuo Yu (2005) "Protein database searches using compositionally adjusted substitution matrices", FEBS J. 272:5101-5109.

Other reports: [Search Summary](#) [\[Taxonomy reports\]](#) [\[Multiple alignment\]](#) [new](#)[Search Parameters](#)**Search parameter name** **Search parameter value**

Program	blastp
Word size	3
Expect value	10
Hitlist size	100
Gapcosts	11,1
Matrix	BLOSUM62
Filter string	F

Genetic Code	1
Window Size	40
Threshold	11
Composition-based stats	2

Karlin-Altschul statistics

**Params** **Ungapped** **Gapped**

Lambda	0.318991	0.267
K	0.133935	0.041
H	0.404134	0.14

Results Statistics

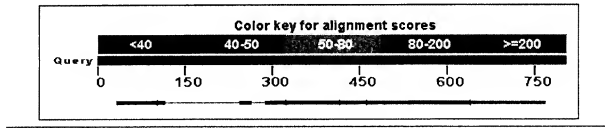
**Results Statistics** parameter name **Results Statistics** parameter value

Effective search space	595935
------------------------	--------

[Graphic Summary](#)
**Distribution of 12 Blast Hits on the Query Sequence**

[?]

An overview of the database sequences aligned to the query sequence is shown. The score of each alignment is indicated by one of five different colors, which divides the range of scores into five groups. Multiple alignments on the same database sequence are connected by a striped line. Mousing over a hit sequence causes the definition and score to be shown in the window at the top, clicking on a hit sequence takes the user to the associated alignments. New: This graphic is an overview of database sequences aligned to the query sequence. Alignments are color-coded by score, within one of five score ranges. Multiple alignments on the same database sequence are connected by a dashed line. Mousing over an alignment shows the alignment definition and score in the box at the top. Clicking an alignment displays the alignment detail.



Dot Matrix View: **Plot of lcl|40585 vs 40587 [?]**

This dot matrix view shows regions of similarity based upon the BLAST results. The query sequence is represented on the X-axis and the numbers represent the bases/residues of the query. The subject is represented on the Y-axis and again the numbers represent the bases/residues of the subject. Alignments are shown in the plot as lines. Plus strand and protein matches are slanted from the bottom left to the upper right corner, minus strand matches are slanted from the upper left to the lower right. The number of lines shown in the plot is the same as the number of alignments found by BLAST.

Descriptions

Sequences producing significant alignments:	Score (Bits)	E Value
lcl 40587 unnamed protein product	57.8	3e-12

Alignments Select All Get selected sequences Distance tree of results Multiple alignment NEW

>lcl|40587 unnamed protein product  
Length: 820

Score = 57.8 bits (138), Expect = 3e-12, Method: Compositional matrix adjust.  
Identities = 45/165 (27%), Positives = 72/165 (43%), Gaps = 28/165 (16%)

Query 634	DQGDYVCSAQDDKTKRHLVQLIILERMA--PMTGNLE-NQTTTIGETTIEVTCPASG	690
D+G+Y C +++ H QL ++ER P++ L N+T +G +E C		
Sbjct 224	DKGNYTCIVENEYGSINHTY--QLDVVERSPHRPIQLAGLPANKTVALGSNVEFMCKVYS	281
Query 691	NPTPHITWKDNET-----LVEDSGIYLRLDGNRN-ITIRRVRKEDGGLYTC	735
+P PHI W K E	+++ +G+ D L +R V ED G YTC	
Sbjct 282	DPQPHIQWLKHIEVNNGSKIGPDNLPPYQILKTAGVNNTTDKEMEVVLHRLRNVSFEDAGEYTC	341
Query 736	QACNVLGCARAET-LFIIEGAQKETN-----LEVIIVLGVTAII	772
A N +G + L +E +E+	LE+II A +	
Sbjct 342	LAGNSIGLSSHNSAWLTVLEALEERPAVMTSPLYLEIIIYCTGAFL	386

Score = 41.6 bits (96), Expect = 2e-07, Method: Compositional matrix adjust.  
Identities = 34/148 (22%), Positives = 62/148 (41%), Gaps = 8/148 (5%)

Query 325	RVHTKPFIAFGSGMKSLSVATVGSQLV-RIPIVKYLSYPAPDIKWYRNGRPIESNN----YT	378
R+ P+ M+ + A + V+ P P +W +NG+ + + Y		
Sbjct 148	RMPVAPYWTSPKMEKKLHVAPAAKTVKFKPSSGTNPTRLWLNGKEFKPDHRRIGGYK	207
Query 379	MIVGDELTIME-VTERDAGNTVILTNPISEMKSHMVSLVVNVPPQICEKALISPMNSY	437
+ IM+ V D GNTY I+N + + + +V P + +A + +		
Sbjct 208	VRYATWSIIMDSVVPSPDKGNYTCIVENEYGSINHTYQLDVVERSPHRPIQLAGLPANKTV	267
Query 438	QVGTMTLCTVYANPPLHHIQWYQLE 465	
G+ C VY++ P HIOW +E		
Sbjct 268	ALGSNVEFMCKVYSD-PQPHIQWLKHIE 294	

Score = 39.7 bits (91), Expect = 6e-07, Method: Compositional matrix adjust.  
Identities = 36/152 (23%), Positives = 64/152 (42%), Gaps = 32/152 (21%)

Query 293	TLTIESVTSDQGEYTCVASSGRMIKRNRFTV-----RVHTKPFIAFGSGMKSLSVATVG	347
+ +SV SD+G YT+ + N T+ R +P + +G+ + +G		
Sbjct 214	SIIMDSVVPSPDKGNYTCIVEN-EYGSINHTYQLDVVERSPHRPIQLAGLPANKTV	270
Query 348	SQVRIPVKYLSSYPAPDIKWYRNGRPIESNYTMIVGDELTIMEVTE-----	392
S V K S P P I+W + IE N + I D L + + +		
Sbjct 271	SNVEFMCKVYSDPQPHIQWLKH--IEVNGSKIGPDNLPPYQILKTAGVNNTTDKEMEVVLH	327
Query 393	-----RDAGNYTVILTNPISEMKQSHMVSLV 418	

DAG YT + N I + S +++++  
 Sbjct 328 LRVNSFEDAGEYTCLAGNSIGLSSHSAWLTVL 359

Score = 38.9 bits (89), Expect = 1e-06, Method: Compositional matrix adjust.  
 Identities = 20/67 (29%), Positives = 31/67 (46%), Gaps = 3/67 (4%)

Query 679 GETIVTCAGNPTPHTWKDNELTIVED---SGTVLRLDGNNRLTIRRRVRKEDGGLYTC 735  
 +T++ CP+SG P P + W K+ + D G +R ++ V D G YTC  
 Sbjct 171 AKTVFKCPSSGTNPTRLWLNGKEFKPDHRIGGYKVRYATWSIIMDSVPSDKGNYTC 230

Query 736 QACNVLG 742  
 N G  
 Sbjct 231 IVENEYG 237

Score = 33.5 bits (75), Expect = 5e-05, Method: Compositional matrix adjust.  
 Identities = 59/306 (19%), Positives = 109/306 (35%), Gaps = 53/306 (17%)

Query 364 IKWYRNGRPI-ESNYTMOVGEDELTIMEVTERDAGNYTIVTLNTPISMEKQSHMVSLLVVNPV 422  
 I W +R+ ESN T I G+E+ + + D G Y + ++P S VNV  
 Sbjct 64 INWL RDGVQLAESNRTRITGEEVEVQDSVPADSGLYACVTSSP---SGSDTTYFSVNVS 119

Query 423 PQIGEKALISPMSNYQYGTMLTCTVYANPPLHHIQWYQWLEEAACSYR-----  
 + + + + + + P + YW E +  
 Sbjct 120 DALPSSEDDDDDDDSSSEEKEETDNTKPNRMRP---VAPYWTSPKEMKKLHAVPAAKTVK 175

Query 472 ---PCTSPDYACKEW-RHVEDFQGGNKIEVTNKQYALIEGKNTVSTLVIQAAANVS--AL 525  
 P +P W ++ +F+ ++I K +YA + + + + + S  
 Sbjct 176 FKCPSSGTNPTRLWLNGKEFKPDHRIGGYKVRYA-----TSIIMDSVPSDKGN 227

Query 526 YKECAINKGRGERVISFHVI-ROPEITVOPAQPTEQ----ESVSLLLCTADRNTFENL 579  
 Y C N+ G V+ R P + A P + +V +C + + +  
 Sbjct 228 YTCIVENEYGSIHNTYQLDVVERSPHRPILOQALPANKTVALGSNEFMCKVYSDPQPHI 287

Query 580 TWYKLGSQATSVHM---GESLTPVCKNLDAWLKLNGTMFSNSTDILIVAFQNALQDQG 636  
 W K H+ G + P NL + L + + + + + + + N S +D G  
 Sbjct 288 QWLK-----HIEVNGSKIGP--DNLPYVQILKTAGVNNTTDKEMEVVLHLRNVSFEDAG 337

Query 637 DVCSA 642  
 +Y C A  
 Sbjct 338 EYTCLA 343

Score = 24.6 bits (52), Expect = 0.021, Method: Compositional matrix adjust.  
 Identities = 10/36 (27%), Positives = 20/36 (55%), Gaps = 0/36 (0%)

Query 291 LSTLTIESVTSDOGEYTCVASSGRMIKRNRTFVVR 326  
 + L + +V+ D GEYCT+A + + + + + V  
 Sbjct 323 MEVHLRLRNVSFEDAGEYTCLAGNSIGLSSHSAWLT 358

Score = 21.6 bits (44), Expect = 0.21, Method: Compositional matrix adjust.  
 Identities = 19/75 (25%), Positives = 29/75 (38%), Gaps = 12/75 (16%)

Query 49 LQITCRQRGD---LDWLWPNAQRDSEERVLVTECGGGDSIFCKTTLTIPRVVGNDTGAYKC 105  
 LQ+ CR + D +WL Q R +T G+ + + + D+G Y C  
 Sbjct 51 LQLRCRRLRDVQSIWLRDGVQLAESNRTRIT---GEEV----EVQDSVPADSGLYAC 101

Query 106 SYRDVDIASTVVYYV 120  
 + T Y V  
 Sbjct 102 VTSSPSGSDDTYFSV 116

Score = 21.2 bits (43), Expect = 0.27, Method: Compositional matrix adjust.  
 Identities = 11/40 (27%), Positives = 16/40 (40%), Gaps = 2/40 (5%)

Query 696 ITWFKDNELTVEWDGIVLRLDGNNRLTIRRRVRKEDGGLYTC 735  
 I W +D L E + R + ++ D GLY C  
 Sbjct 64 INWL RDGVQLAESNR---RITGEEVEVQDSVPADSGLYAC 101

Score = 18.9 bits (37), Expect = 1.4, Method: Compositional matrix adjust.  
 Identities = 9/22 (40%), Positives = 13/22 (59%), Gaps = 2/22 (9%)

Query 247 NCTARTELNLVGLDFWTWHSPSK 268  
 NCT EL + + WH+ PS+  
 Sbjct 722 NCT---NELYMMRDCWHAVPSQ 741

Score = 18.9 bits (37), Expect = 1.4, Method: Compositional matrix adjust.  
Identities = 6/16 (37%), Positives = 8/16 (50%), Gaps = 0/16 (0%)

Query 468 CSYRPQGQTSPYACKEW 483  
C+ RP T P + W  
Sbjct 19 CTARPSPTLPRQAQPW 34

Score = 18.1 bits (35), Expect = 2.2, Method: Compositional matrix adjust.  
Identities = 18/75 (24%), Positives = 29/75 (38%), Gaps = 12/75 (16%)

Query 37 QKDLTILATTQLQITCRG---QRDLDWLWPNAQRDSEERVLVTECGGGDSIFCKTLTI 92  
+K + + A T++ C L WL + + R+ GG + T + I  
Sbjct 162 EKKLHAVPAAKTVKPKCPSSQTPNPTLRWLKNNGKEPKPDHRI-----GGYKVRYATWSI 215

Query 93 --PRVVGNDTGAYKC 105  
VV +D G Y C  
Sbjct 216 IMDSVVPSDKGNYTC 230

Score = 16.5 bits (31), Expect = 6.2, Method: Compositional matrix adjust.  
Identities = 6/12 (50%), Positives = 8/12 (66%), Gaps = 0/12 (0%)

Query 673 NOTTTIGETIEV 684  
N+T GE +EV  
Sbjct 77 NRTRITGEEVEV 88

Select All [Get selected sequences](#) [Distance tree of results](#) [Multiple alignment](#) [New](#)